

Research Paper

# Dot to dot: high- $z$ little red dots in $M_{\text{bh}}-M_{\star}$ diagrams with galaxy-morphology-specific scaling relations and nuclear star clusters

Alister W. Graham<sup>1</sup>, Igor V. Chilingarian<sup>2</sup>, Di u D. Nguy n<sup>3</sup>, Roberto Soria<sup>4,5</sup>, Mark Durr 1, and Duncan A. Forbes<sup>1</sup>

<sup>1</sup> Centre for Astrophysics and Supercomputing, Swinburne University of Technology, Hawthorn, VIC 3122, Australia.

<sup>2</sup> Smithsonian Astrophysical Observatory, 60 Garden St. MS09, Cambridge, MA 02138, USA.

<sup>3</sup> Universit  de Lyon 1, ENS de Lyon, CNRS, Centre de Recherche Astrophysique de Lyon (CRAL) UMR5574, F-69230 Saint-Genis-Laval, France.

<sup>4</sup> INAF-Osservatorio Astrofisico di Torino, Strada Osservatorio 20, I-10025 Pino Torinese, Italy.

<sup>5</sup> Sydney Institute for Astronomy, School of Physics A28, The University of Sydney, Sydney, NSW 2006, Australia.

## Abstract

High-redshift ‘little red dots’ (LRDs) detected with the *James Webb Space Telescope* are considered the cores of emerging galaxies. For the first time, we compare LRDs in  $M_{\text{bh}}-M_{\star}$  diagrams with an array of  $z = 0$  galaxy-morphology-dependent scaling relations, along with the  $M_{\text{bh}}-M_{\star,\text{nsc}}$  relation for nuclear star clusters. The  $M_{\text{bh}}-M_{\star,\text{sph}}$  relations for spheroidal stellar systems are characterised by a nearly parallel set of quasi-quadratic (or steeper) distributions that are known to trace the ‘punctuated equilibrium’ of galaxies, reflecting their stepwise growth in black hole mass and merger-built bulge/spheroid mass. We show that LRDs are not equivalent to nuclear star clusters, with the latter having higher  $M_{\text{bh}}/M_{\star}$  ratios. However, the least massive LRDs exhibit similar  $M_{\text{bh}}$  and  $M_{\star,\text{gal}}$  values as ultracompact dwarf (UCD) galaxies. We show that the LRDs span the  $M_{\text{bh}}-M_{\star,\text{gal}}$  diagram from UCD galaxies to primaeval lenticular galaxies. In contrast, spiral galaxies and the subset of major-merger-built early-type galaxies define offset relations. Additionally, we observe that low- $z$  galaxies with active galactic nuclei align with the steep black hole scaling relations for disc galaxies defined by primarily inactive galaxies with directly measured black hole masses. Collectively, this highlights the benefits of considering galaxy morphology, which reflects their accretion and merger history, to understand the coevolution of galaxies and their black holes.

**Keywords:** galaxies: bulges, galaxies: elliptical and lenticular, cD, galaxies: structure, galaxies: interactions, galaxies: evolution, (galaxies:) quasars: supermassive black holes

(Received 15 December 2024; revised xx xx xxxx; accepted xx xx xxxx)

## 1. Introduction

After 3C 273 was determined to be receding at 1/6th the speed of light ( $z = 0.158$ ; Schmidt 1963), Schmidt’s quasars have been found at ever-increasing redshifts. Izumi et al. (2021) report on over 40 low- and high-luminosity quasars<sup>a</sup> and quasi-stellar objects (QSOs) at  $z \gtrsim 6$ . While QSOs are predominantly blue, it is recognised that some dust-reddened active galactic nuclei (AGN) may have been overlooked in the past (e.g. Fall & Pei 1993; Webster et al. 1995; Stickel et al. 1996). In addition to the sample of possible AGN at  $5 < z < 9$  presented by Akins et al. (2024), recent records include an AGN at  $z = 8.50$  (Kokorev et al. 2023), the QSO CEERS.1019 at  $z = 8.7$  (Larson et al. 2023), and GNz11 (Maiolino et al. 2023, 2024; Bunker et al. 2023). Due to their

appearance in *James Webb Space Telescope* (JWST) images<sup>b</sup>, these recently detected ( $4 \lesssim z \lesssim 10$ ) AGN have been dubbed ‘little red dots’ (LRDs; Barro et al. 2024; Bogd n et al. 2024; Matthee et al. 2024; P rez-Gonz lez et al. 2024; Yue et al. 2024).<sup>c</sup>

For years, it was reported (e.g. Bennert et al. 2011; Wang et al. 2013; Park et al. 2015; Venemans et al. 2016; Decarli et al. 2018; Ding et al. 2020; Pensabene et al. 2020) that high- $z$  AGN reside above the original near-linear  $z \sim 0$   $M_{\text{bh}}-M_{\star}$  relation (Magorrian et al. 1998). This was regarded as evidence that, over time, the galaxies’ stellar populations must play catch-up to the supermassive black holes (SMBHs) for the systems to arrive at the  $z \approx 0$  relation. However, at least two factors were confounding the veracity of whether or not any evolution in the SMBH mass - host spheroid or galaxy stellar mass ( $M_{\text{bh}}-M_{\star}$ ) scaling with redshift had been detected. The first was that the  $z \sim 0$   $M_{\text{bh}}-M_{\star}$  relation is not linear. For gas-rich systems, such as spiral (S) galaxies and (wet merger)-built lenticular (SO) galaxies, the  $M_{\text{bh}}-M_{\star}$  relation is much steeper than linear (Graham 2012; Graham & Scott 2013;

**Author for correspondence:** A.W. Graham, Email: AGraham@swin.edu.au

**Cite this article:** Graham A.W., Chilingarian I.V., Nguy n D.D., Soria R., Durr  M., Brodie, J.P., Forbes, D.A. (2024) Comparing high- $z$  ‘little red dots’ to nuclear star clusters, ultracompact dwarf galaxies, primaeval  $z \sim 0$  lenticular galaxies, and more in the  $M_{\text{bh}}-M_{\star}$  diagram. *Publications of the Astronomical Society of Australia* 00, xxx–xxx. <https://doi.org/10.1017/pasa.xxxx.xx>

<sup>a</sup>Quasi-stellar radio sources (quasars) have strong radio emission, while QSOs do not.

<sup>b</sup>These nascent galaxies are sometimes spatially resolved (Rinaldi et al. 2024). However, a comparison of LRDs with UCDs in the size-mass diagram is left for a follow-up paper once more LRD sizes become available.

<sup>c</sup>Some LRDs, but more likely globular clusters, may have started life as the ‘little blue dots’ (LBDs) found by Elmegreen & Elmegreen (2017). The absence of an AGN in these distant LBDs would further distinguish them from the LRDs.

Scott et al. 2013). These observations were reviewed and explained by Graham (2016b) in terms of consistency with the (stellar luminosity,  $L$ )-(central stellar velocity dispersion,  $\sigma$ ) relations. For the S galaxies, Savorgnan et al. (2016) presented the steep ‘blue sequence’ suggested in the data of Salucci et al. (2000) and better quantified by Davis et al. (2018, 2019). Consequently, selecting QSOs in massive gas-rich galaxies at high redshifts will sample the upper end of a steep non-linear relation and, therefore, sample from above the reported near-linear  $z \sim 0$  relation. In this case, the apparent higher  $M_{\text{bh}}/M_*$  ratios measured at higher redshift need not imply that there has been any evolution. This scenario can be appreciated by looking at Izumi et al. (2021, their figure 13) and Kocevski et al. (2023, their figure 9). These authors correctly noticed that the trend in the  $M_{\text{bh}}-M_*$  diagram was due to luminosity bias in past samples of high- $z$  AGN. However, they missed the connection/explanation with the quadratic or steeper  $M_{\text{bh}}-M_*$  relation.

The second issue has been the need for more attention to galaxy components and morphology. As stressed previously (e.g. Sahu et al. 2019),  $M_{\text{bh}}-M_*$  scaling relations defined by grouping all galaxy types, or even just the early-type galaxies (ETGs), will be misleading. The slope and zero-point calibration of such relations will depend on the random number of specific galaxy types in one’s sample. For example, not only did Davis et al. (2018) and Davis et al. (2019) define the steep relations for the S galaxies, but reported relations for all ETGs depend on the arbitrary fraction of primordial/primaeval<sup>d</sup> S0 galaxies (Graham 2023c) versus wet-major-merger-built S0 galaxies, and the number of ellicular (ES)<sup>e</sup> and elliptical (E) versus brightest cluster galaxies (BCGs) built from multiple major mergers). To fully address the topic of galaxy/black hole coevolution, one requires knowledge of the galaxy-morphology-dependent  $M_{\text{bh}}-M_*$  relations that have progressively advanced over the last dozen years or so.

The  $M_{\text{bh}}-M_{*,\text{gal}}$  diagram in Graham (2023c, figure A4) reveals several different distributions. There are the dust-poor S0 galaxies with little-to-no evidence of past merger activity, which are likely preserved primaeval galaxies that need never have displayed a spiral pattern. There are the S galaxies (that experience gas accretion, recycling of gas through stellar winds not ablated by ram pressure stripping from an X-ray-hot halo, and minor-to-substantial mergers with satellites and other galaxies). Third, there are the (major merger)-built ETGs forming from gas-rich mergers involving S galaxies to produce dust-rich S0 galaxies, and relatively gas-poor mergers of high-mass S0 galaxies to produce discless E galaxies, and so on to the BCGs.

There is an additional population of ultracompact dwarf (UCD) galaxies (e.g. Harris et al. 1995; Hilker et al. 1999; Drinkwater et al. 2000; Phillipps et al. 2001; Madrid et al. 2010; Brodie et al. 2011; Chilingarian et al. 2011; Pfeffer & Baumgardt 2013; Forbes et al. 2020; Graham 2020). These are considered to be the remnant nuclei of threshed low-mass disc galaxies (Zinnecker et al. 1988; Bekki et al. 2001; Drinkwater et al. 2003), composed of the inner dense compact nuclear star cluster (NSC) from the progenitor galaxy and some residual galaxy stars forming a larger secondary component. NSCs and the inner components of UCDs occupy a similar distribution in the  $M_{\text{bh}}-M_{*,\text{sph}}$  diagram (Graham 2020). They are, however, often excluded from  $M_{\text{bh}}-M_*$  scaling diagrams. Here, we plot the central massive black hole mass versus the stellar mass of NSCs, the inner component of UCDs,

the bulge component of disc galaxies, and the spheroidal component of E galaxies. We additionally plot black hole mass versus the total stellar mass of NSCs and UCDs, along with all galaxies with directly measured black hole masses. Several samples of local AGN have also been added, along with recently published data for LRDs.

Assuming the recent deep *JWST* data has been correctly interpreted<sup>f</sup> and the associated redshifts and (SMBH and stellar) masses broadly hold (they may not: Ostriker & Heisler 1984; Ananna et al. 2024; Yue et al. 2024; Leung et al. 2024) (but see Juodžbalis et al. 2024; Pacucci & Narayan 2024), then these new higher-redshift ( $7 < z < 11$ ) LRDs/AGN with particularly high  $M_{\text{bh}}/M_*$  ratios offer compelling evidence that the growth of the stellar body of a galaxy does play catch-up to the SMBH. Some of these LRDs have  $M_{\text{bh}}/M_*$  ratios orders of magnitude higher (Pacucci et al. 2023, their figure 2) than ‘ordinary’ local galaxies that define the Jeans-Reynolds-Hubble sequence (Jeans 1919; Reynolds 1925; Hubble 1926, 1936). This would imply a kind of inside-out formation in which a dense star cluster or the inner parts of a galaxy form before the larger disc, with the massive black hole established early on. Graham (2024b) noted that these LRDs might be somewhat akin to UCDs with NSCs.<sup>g</sup>

The steep galaxy-morphology-dependent  $M_{\text{bh}}-M_*$  relations, which differ dramatically from the near-linear Magorrian et al. (1998) relation, are also included here for an insight into the coevolution of galaxies and black holes. These relations have already delivered considerable advances on many fronts. They led to the establishment of the ‘Triangal’, a successor to the Tuning Fork diagram (Jeans 1928; Hubble 1936), the van den Bergh (1976) Trident, and the ATLAS<sup>3D</sup> comb (Cappellari et al. 2011) due to the Triangal’s recognition of different types of S0 galaxy and the inclusion of evolutionary pathways absent from the other schemes.<sup>h</sup> The set of relations further revealed that many S0 galaxies are neither faded (Spitzer & Baade 1951; Gunn & Gott 1972) nor merged S galaxies (Toomre 1977; Roos & Norman 1979; Gerhard 1981; Negroponte & White 1983) but primaeval (Graham 2023b). The relations have additionally (i) resulted in greater recognition of the importance of major galaxy mergers (Graham & Sahu 2023a,b; Graham 2023a; Graham et al. 2024) relative to suspected AGN feedback, (ii) revealed that a large number of hierarchical mergers, leading to the central limit theorem establishing a linear  $M_{\text{bh}}-M_*$  relation (Peng 2007; Jahnke & Macciò 2011), is not applicable<sup>i</sup>, (iii) revealed that galaxy morphology (reflective of a galaxy’s accretion/merger history) better dictates the specific star formation rate (Graham et al. 2024) than either the bulge mass or bulge-to-disc stellar mass ratio (e.g. Martig et al. 2009) or AGN feedback as measured by the specific black hole mass ( $M_{\text{bh}}/M_*$ : Terrazas et al. 2016, 2017), (iv) illuminated the paths of galaxy speciation (Graham 2023c), and (v) better revealed often-overlooked sequences and patterns in the colour-magnitude/(stellar mass) diagram (CMD: de Vaucouleurs & de Vaucouleurs 1972; Graham 2024a). The latter included confirming the presence of a green mountain (Eales et al. 2018) and range (Schweizer & Seitzer 1992) and adding to popular evolutionary pathways in the CMD (e.g. Schawinski et al. 2014) that had not previously encapsulated primaeval S0 galaxies.

Section 2 introduces the various data sets that appear in the  $M_{\text{bh}}-M_{*,\text{sph}}$  and  $M_{\text{bh}}-M_{*,\text{gal}}$  diagrams presented herein. Nearby galaxies with

<sup>d</sup>The term ‘primaeval’ is used here to refer to the first type of galaxy to form prior to subsequent significant merger events that change the galaxy type. This is expected to be a disc galaxy due to the conservation of angular momentum in the contracting gas clouds (Evrard et al. 1994), which need not but may be clumpy at high- $z$  (Mowla et al. 2024).

<sup>e</sup>Liljer (1966) introduced the ‘ES’ galaxy nomenclature for ETGs with intermediate-scale discs that do not dominate the light at large radii. Graham et al. (2016b) introduced the name ‘ellicular’.

<sup>f</sup>Langeroodi & Hjorth (2023) report that some LRDs are brown dwarf stars.

<sup>g</sup>AWG discussed LRDs overlapping (connecting?) with UCDs (and NSCs) at the July 2024 conferences <http://cosmicorigins.space/smbh-sexten> and <https://indico.ict.inaf.it/event/2784/>.

<sup>h</sup>This evolution includes mergers of S galaxies evolving into S0 galaxies without needing to transition through a population of disc galaxies with weak spiral patterns, as with the Trident (van den Bergh 1976) and Comb (Cappellari et al. 2011).

<sup>i</sup>The theorem, *per se*, is correct, but the actual number of mergers has not been sufficiently large for the theorem to apply.

directly measured black hole masses, including UCDs (Section 2.1.1), along with samples of low- $z$  AGN (Section 2.2.1) and high- $z$  AGN, including LRDs (Section 2.2.2), have representation. In Section 3, we discuss the  $M_{\text{bh}}-M_*$  diagrams. We start with a short recap of developments over the past decade (Section 3.1), breaking away from the original near-linear relations (e.g. Dressler & Richstone 1988; Dressler 1989; Kormendy & Richstone 1995; Graham 2007, and references therein) defined by predominantly ETGs. In addition to advances using relations not based on one-fit-for-all types of galaxy, which are skewed/biased by the random fractions of ETGs and late-type galaxies (LTGs, i.e. S galaxies), in one’s sample, we discuss how not grouping the different ETGs has similar benefits for avoiding a biased relation and revealing valuable scientific information. Section 3.2 discusses the LRDs and their distribution in the  $M_{\text{bh}}-M_*$  diagrams. Finally, Section 3.3 describes the location of lower- $z$  AGN in the diagrams, revealing that they follow the steep relations defined by local galaxies with predominantly inactive black holes. A concise summary is given in Section 4

## 2. Data

### 2.1. (Predominantly) inactive stellar systems

#### 2.1.1. Galaxies with directly measured black hole masses

A local ( $z \sim 0$ ) sample of predominantly inactive (i.e. not QSO) galaxies with directly measured SMBH masses is described in a recent series of papers spanning Graham & Sahu (2023a) to Graham (2024b). Multicomponent decompositions of the galaxy images from the *Spitzer Space Telescope* (SST) were performed, separating inner discs (e.g. Scorza & van den Bosch 1998; Balcells et al. 2007; Savorgnan & Graham 2016a; Davis et al. 2019; Sahu et al. 2019) and bar-induced (X/peanut shell)-shaped structures (e.g. de Vaucouleurs & de Vaucouleurs 1972; Ciambur & Graham 2016) from bulges. Bars, rings, and ansae were modelled. In addition to the single exponential disc model, truncated and anti-truncated disc models were used, as were inclined disc models as required. Using the appropriate disc model prevents undermining the bulge (and other components’) flux. For example, major-merger-built S0 galaxies tend to have anti-truncated discs, as reported by Graham (2024b). Using a single exponential model in such galaxies would, therefore, compromise the derivation of the bulge luminosity and, consequently, stellar mass. Graham (2023b, section 4.3.2) suggests that the low-mass dust-poor (primarily primaeval) S0 galaxies, in contrast, might tend to have truncated discs, a discovery that will be detailed elsewhere.

The absence from this sample of galaxies with (directly measured black hole masses and)  $M_{*,\text{sph}} \lesssim 2 \times 10^9 M_\odot$  and  $M_{*,\text{gal}} \lesssim 10^{10} M_\odot$  is an observational bias due to difficulties measuring their central black hole mass. However, galaxies with lower stellar masses of course exist, as seen in, for example, the colour- $M_{*,\text{gal}}$  diagram of Graham (2024a, figure 5), and are increasingly reported with directly measured SMBH masses. These additional galaxies are individually named in the diagrams and plotted with a different (cyan) symbol because they were not used to derive the scaling relations shown there.

The ETGs were separated into BCGs, E and ES galaxies (Graham & Sahu 2023b), and S0 galaxies that were further separated into dust-poor and dust-rich, which is a good indicator of their origin as either primaeval (no major mergers, likely stripped of gas due to ram-pressure and thus ‘preserved’ but with an ageing stellar population)<sup>j</sup> or built

from a wet major merger event likely involving an S galaxy (Graham 2023b,c). These latter dust-rich systems, presumably with considerable neutral hydrogen gas content, are also big galaxies with massive black holes that do not remove their gas on short timescales. For example, the dusty S0 galaxy Fornax A is a 3-Gyr-old merger product with  $\sim 10^9 M_\odot$  of HI gas (Serra et al. 2019). However, not all major merger remnants retain a dusty appearance.

In Graham (2024b), NGC 4697, NGC 3379, NGC 3091, and NGC 4649 were reclassified as S0 rather than E galaxies, with the adjustment supported by kinematic maps of the galaxies. Although not dust-rich, all but NGC 3091 — the brightest galaxy in Hickson Compact Group No. 42 — are recognised mergers in the literature. As detailed in Graham (2024b), their anti-truncated discs are also likely a signature of their merger origin. Two other S0 galaxies are regarded here as major-merger remnants, although they too are not classified (see Graham 2023b) as dust-rich (i.e. dust=Y, that is, a strong yes).<sup>k</sup> The first is NGC 5813<sup>l</sup> (dust=y, widespread but weak) (Hopp et al. 1995; Krajnović et al. 2015). Although not (and probably more correctly “no longer”) dust-rich, NGC 5813 is an old merger surrounded by a group-sized hot gas halo (Randall et al. 2015) that destroys dust, removes gas, and thereby inhibits star formation, preferentially impacting lower-mass galaxies. The second is NGC 7457 (dust=N, that is, a strong no) with cylindrical rotation about its major axis, revealing that it, too, experienced a merger, determined via other means to have occurred 2-3 Gyr ago (Sil’chenko et al. 2002; Chomiuk et al. 2008; Hargis et al. 2011; Molaeinezhad et al. 2019). NGC 7457 displays an anti-truncated stellar disc and is somewhat unusual in that it is a merger that has lost its dust. However, this is plausible given its relatively low galaxy stellar mass of around  $10^{10} M_\odot$  compared to  $\sim 10^{11} M_\odot$  for the dust-rich merger-built S0 galaxies. Finally, two ES,b galaxies (NGC 5845 and NGC 1332, with dust=n, that is, only nuclear dust) are *suspected* major merger remnants given their embedded intermediate-scale discs, as noted in Section 3.3.

While the following S0 galaxies are not considered to have been built by a major merger and are not dust-rich, they have, however, experienced a minor merger or accretion event, leaving them still largely ‘primaeval’ in the sense of their stellar mass and structure, having not mutated into an S galaxy (Julian & Toomre 1966; D’Onghia et al. 2013; Graham 2023c). They are NGC 2787, NGC 3998, and NGC 4026 (all three categorised as dust=y), and NGC 1023, NGC 4762, and NGC 7332 (all three with dust=N). References to works discussing the merger history of these galaxies are provided in Graham (2023b, table 2).

For those thinking there is a lot to keep up with, we do not disagree. The notion that S0 galaxies are only faded or merged S galaxies (e.g. see the discussion of the colour-mass diagram by Schawinski et al. 2014) has been supplanted with the recognition of an additional S0 population from which the S galaxies formed. The high  $M_{\text{bh}}/M_{*,\text{sph}}$  ratios of these initial S0 galaxies, and their location in the  $M_{\text{bh}}-M_*$  diagrams, is what ruled out the previous two (faded or merged S galaxy) formation channels for this population of S0 galaxies. This revelation has also resulted in re-drawing the evolutionary paths in the colour-mass diagram (Graham 2024a). How the LRDs relate with this explicitly identified primaeval population is explored, for the first time, in this work.

<sup>k</sup>The four dust ‘bins’ (Y, y, n, N) were introduced and are described in Graham (2023b).

<sup>l</sup>The potentially depleted stellar core in NGC 5813 (Richings et al. 2011; Dullo & Graham 2014) is thought to be formed from the merger of a binary black hole (Begelman et al. 1980; Graham 2004). However, it may be worth remodelling this galaxy with an anti-truncated disc to check if the simpler Sérsic bulge model will suffice once this is implemented.

<sup>j</sup>Given their coincident location in the  $M_{\text{bh}}-M_{*,\text{sph}}$  diagram with S galaxies, a small handful of dust-poor S0 galaxies in the sample may be the gas-stripped and faded S galaxies proposed by Gunn & Gott (1972) and Davies & Lewis (1973).



### 2.1.2. UCDs and NSCs

A local sample of UCDs and NSCs with directly measured SMBH masses has come from Graham & Spitler (2009) and Graham (2020, and references therein).<sup>m</sup> This sample includes the SMBH and NSC masses for the (stellar-stripped S0 and now) cE galaxy M32 (Nguyen et al. 2018) and the flattened ‘peculiar’<sup>n</sup> dwarf ETG NGC 205 (Nguyen et al. 2019), plus an updated black hole mass for NGC 404 (Davis et al. 2020)<sup>o</sup> and NGC 4395 (Brum et al. 2019).<sup>p</sup> The sample is supplemented with NGC 5102 and NGC 5206 (Nguyen et al. 2018, 2019).<sup>q</sup> The SMBH-NSC mass for NGC 3593 (Nguyen et al. 2022) has also been added, as has the globular clusters B023-G078 around M31 (Pechetti et al. 2022) and  $\omega$  Centauri (D’Souza & Rix 2013; Häberle et al. 2024) for which the *Gaia*-Sausage/Enceladus host galaxy mass is used (Lane et al. 2023), as discussed by Limberg (2024). Finally, the dwarf spheroidal galaxy Leo I (Mateo et al. 2008) has been included, although it may not contain a massive black hole (Pascale et al. 2024).

The original  $M_{\text{bh}}-M_{*,\text{nsc}}$  relation, involving nuclear star cluster masses,  $M_{*,\text{nsc}}$ , was first published in Graham (2016a), having been presented at a 2014 IAU conference in Beijing. The relation was updated by Graham (2020, equation 6) and is shown in Fig. 1, along with the galaxy-morphology-specific  $M_{\text{bh}}-M_{*,\text{sph}}$  relations described earlier. It stems from the discovery of the  $M_{*,\text{nsc}}-M_{*,\text{sph}}$  relation (Balcells et al. 2003; Graham & Guzmán 2003) coupled with the  $M_{\text{bh}}-M_{*,\text{sph}}$  relation and appears to hold until (i) the erosion of the star clusters at high black hole masses due to binary SMBHs (Bekki & Graham 2010; Gualandris & Merritt 2012) or (ii) the appearance of a nuclear disc 10s-to-100s of parsec in size rather than just an ellipsoidal star cluster. To date, the  $M_{\text{bh}}-M_{*,\text{nsc}}$  relation has not received anywhere near the attention of the  $M_{\text{bh}}-M_{*,\text{sph}}$  relation, yet it holds insight into the coevolution of dense star clusters and massive black holes with important consequences for gravitational wave science from extreme mass ratio inspiral (EMRI) events (e.g. Preto & Amaro-Seoane 2010; Mapelli et al. 2012; Babak et al. 2017; Gair et al. 2017; Amaro-Seoane et al. 2023).

For the  $M_{\text{bh}}-M_{*,\text{sph}}$  diagram shown in Fig. 1, the stellar mass of the inner component of the UCDs, i.e. the dense NSC obtained from decompositions of their light profiles, has been plotted. For the  $M_{\text{bh}}-M_{*,\text{gal}}$  diagram (Figures 2 and 3), the total stellar mass of the UCDs has been plotted. This latter approach mirrors the plotting of the total stellar mass for the ‘ordinary’ galaxies shown in Figures 2 and 3, while their bulge or equivalently spheroid stellar mass is plotted in Fig. 1.

## 2.2. AGN with derived black hole masses

### 2.2.1. Low- $z$ AGN

Estimated black hole masses from the compilation of low-redshift ( $z \lesssim 0.2$ ) AGN used by Graham & Scott (2015) are presented in Figures 1 and 2. The black hole mass estimates for the ten AGN from Reines et al. (2013) are reduced here by 0.75 to bring the virial factor used by Reines et al. (2013) in line with Graham et al. (2011). The compilation also includes eleven AGN from Busch et al. (2014), ten AGN from Mathur et al. (2012), two from Yuan et al. (2014), and UM 625 from

Jiang et al. (2013). This sample is bolstered with a further 8 ( $=10-2$ )<sup>f</sup> confirmed AGN with  $0.024 < z < 0.072$  from Chilingarian et al. (2018, their table 2). AGN data from Jiang et al. (2011), with  $2 \times 10^5 \lesssim M_{\text{bh}}/M_{\odot} \lesssim 2 \times 10^6$ , are also included.

In passing, it is noted that Jiang et al. (2013) report that the galaxy UM 625 with an AGN can be convincingly categorised as hosting a pseudobulge due to its blue colour and Sérsic index  $n < 2$ . However, ‘classical’ bulges built from major wet mergers will have lingering star formation (Graham et al. 2024), and their bulges can have  $n < 2$  (e.g. Sahu et al. 2020; Graham 2024b). Moreover, the high bulge-to-total ( $B/T$ ) ratio of 0.6 reported by Jiang et al. (2013) additionally favours a merger origin. UM 625 likely represents an endemic misclassification of bulges, an issue raised by Graham (2014). This situation is reminiscent of that with other dust-rich S0 galaxies built from major wet mergers, such as NGC 1194, NGC 1316, NGC 5018 and NGC 5128, which reside below the old near-linear  $M_{\text{bh}}-M_{*,\text{sph}}$  relation for ETGs but on the steep  $M_{\text{bh}}-M_{*,\text{sph}}$  relation for merger-built (dust-rich) S0 galaxies (Graham 2023b).

It is additionally noted that *galaxy* stellar masses were used for some of the 34 AGN with  $z \sim 0.1$  in the  $M_{\text{bh}}-M_{*,\text{sph}}$  diagram (Fig. 1). Specifically, the galaxies from Yuan et al. (2014) and Reines et al. (2013) were, in the absence of bulge/disc decompositions, effectively taken to be E galaxies. If they are S or S0 galaxies, then the above practice will have acted to shift them rightward in Fig. 1. Such a shift also occurs when using bulge masses if the  $B/T$  ratios of the disc galaxies have been overestimated. This appears to be the situation with the AGN data from Busch et al. (2014) and Mathur et al. (2012) based on the agreement of their AGN sample with the inactive S galaxies in the  $M_{\text{bh}}-M_{*,\text{gal}}$  diagram (Fig. 2).

A second  $M_{\text{bh}}-M_{*,\text{gal}}$  diagram (Fig. 3) has been made with alternate sources of AGN data. This was done, in part, to avoid crowding. The other (main) reason was to provide a diagram that better distinguishes the primaevial S0, S, and merger-built galaxies with directly measured black hole masses. The estimated black hole masses in the AGN from Reines & Volonteri (2015) and the entire sample of 305 intermediate-mass black holes candidates with  $4 \times 10^4 \lesssim M_{\text{bh}}/M_{\odot} \lesssim 2 \times 10^5$  from Chilingarian et al. (2018) are shown in Fig. 3.<sup>5</sup> The SMBH masses from Reines & Volonteri (2015) are reduced here by 0.7 ( $=0.75/1.075$ ) to ensure a consistent virial factor,  $f = 3$ , with the above AGN samples. In addition, data from Lin et al. (2024b) for 59 ‘green peas’<sup>t</sup> with  $z < 0.4$  are shown, as are the  $z \gtrsim 6$  AGN data from Izumi et al. (2021), as noted in the following subsection.

### 2.2.2. High- $z$ AGN and LRDs

Many teams have reported measurements of the stellar mass associated with high- $z$  AGN. Before *JWST* data, Izumi et al. (2018) and Izumi et al. (2021) presented a compilation of AGN at  $6 \lesssim z \lesssim 7$ . They stressed how sample selection bias of bright QSOs at these high redshifts had swayed the conclusions from past investigations. Their compilation rectified this situation by including lower luminosity QSOs at the same high redshifts. Their data compilation is shown here in Fig. 3, although it is noted that the galaxy masses are dynamical rather than stellar, and, as such, smaller symbols have been used for this sample. Their SMBH masses were based on the prescriptions given by Vestergaard

<sup>m</sup>The inner stellar component of M59-UCD3 may be a nuclear disc rather than an NSC.

<sup>n</sup>NGC 205 has dust patches and young stars near its centre (Haas 1998; Marleau et al. 2006).

<sup>o</sup>This mass is questionable as estimates from reverberation mappings suggest a black hole mass that is an order of magnitude smaller (Gu et al. 2024; Pandey et al. 2024).

<sup>p</sup>The nuclear star cluster mass is taken from den Brok et al. (2015).

<sup>q</sup>NGC 5102 and NGC 5206 would benefit from a bulge/disc decomposition rather than the single Sérsic model that has been fit to the main galaxy. The nuclear star cluster, rather than the nuclear star cluster plus nuclear disc, is plotted here. As shown in Balcells et al. (2007), both nuclear components are common in S0 galaxies (e.g. Lyubenova et al. 2013).

<sup>f</sup>J153425.58+040806.7 and J160531.84+174826.1 (from Chilingarian et al. 2018) are already included in the sample from Reines et al. (2013).

<sup>5</sup>Aside from the ten (8+2) AGN from Chilingarian et al. (2018) that are mentioned above and plotted in Fig. 2, just one other AGN (SDSS J122548.86+333248.7) from Graham & Scott (2015) appears in the larger sample from Chilingarian et al. (2018) plotted in Fig. 3.

<sup>t</sup>‘Green peas’ are luminous but low-mass ( $\lesssim 10^{10} M_{\odot}$ ) compact galaxies with substantial star formation (Cardamone et al. 2009).

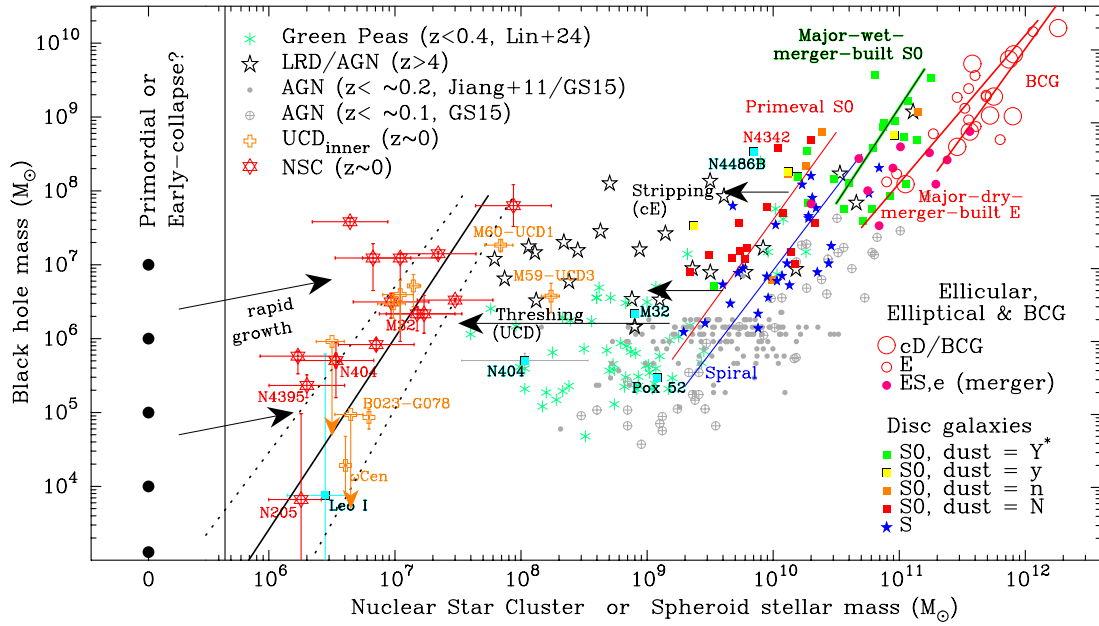


**Figure 1.**  $M_{\text{bh}}-M_{\text{sph}}$  diagram and relations. This is an extension of figure 5 from Graham (2024b), itself an adaption of figure 6 from Graham & Sahu (2023b). From right to left, the lines from the literature are as follows. The right-most red line represents BCGs, and the second-from-right red line represents non-BCG E galaxies (Graham 2024b, table 2), both primarily built from ‘dry’ major mergers. The green line represents ‘wet’ major merger)-built dust-rich (dust=Y) S0 and the Es,b galaxies (Graham 2024b, table 2), hence the asterisk on the Y in the figure legend. Next, the blue line represents S galaxies (Graham 2023c, table 1), while the orange line represents dust-poor (dust=N) S0 galaxies referred to here as primaevael (Graham 2023c, table 1). Stripping and threshing the stars from these galaxies may produce cE and UCD galaxies, respectively. The left-most solid and dotted lines represent the NSCs and inner component of UCDs (Graham 2020, equation 6). Notes: Spheroid masses of AGN with  $4 \times 10^6 \lesssim M_{\text{bh}}/M_{\odot} \lesssim 5 \times 10^7$  have likely been overestimated (in these suspected S galaxies, based on their location in Fig. 2). Without any structural decomposition of the LRDs, their total stellar mass is shown here under the implicit assumption, which we denounce (Section 3.2), that they are spheroidal structures without a disc component. Upper-left legend: Lin+24 = Lin et al. (2024b); ‘LRD/AGN’ covers the LRDs reported in the recent literature, as noted in Section 2; Jiang+11 = Jiang et al. (2011); GS15 = Graham & Scott (2015). The NSC and UCD data come from Graham (2020, and references therein). Lower-right legend: Galaxies with directly measured SMBH masses (Graham & Sahu 2023a), with updates noted in Section 2. Cyan squares (and the green peas and grey AGN samples) are additional galaxies not used to derive the relations.

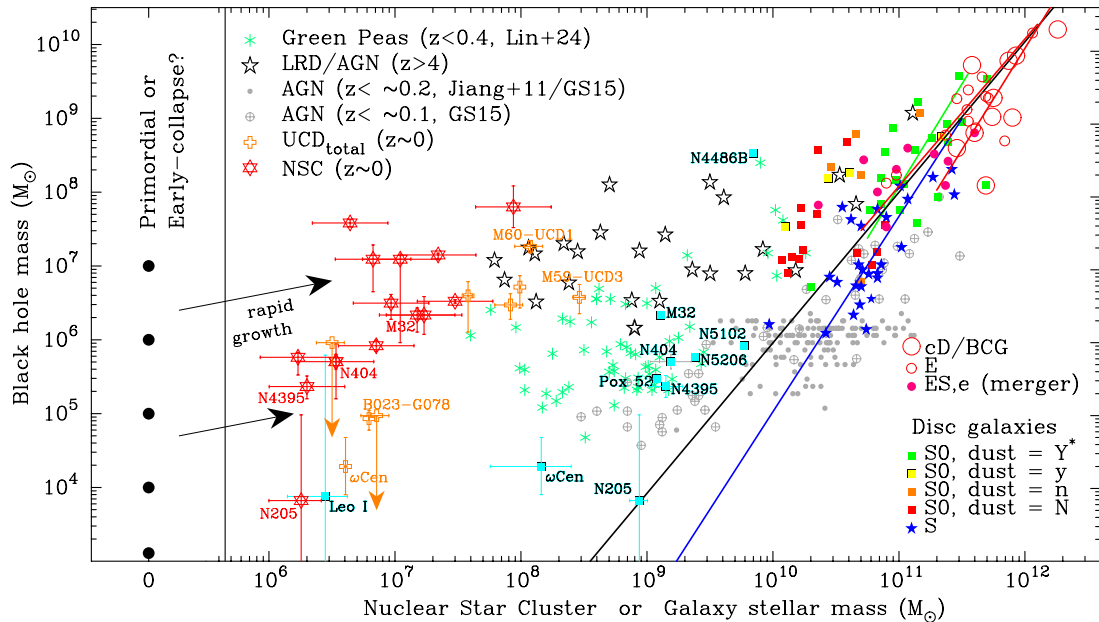


**Figure 2.**  $M_{\text{bh}}-M_{\text{gal}}$  diagram and relations. Modification of Fig. 1, building on figure A4 from Graham (2023c). Here, the inner plus outer components of UCDs are used for their galaxy stellar mass. The right-most red line (upper-right) denotes E BCGs, while the longer red line denotes non-BCG E galaxies (Graham 2024b, table 2) and overlaps with the slightly steeper green line representing dust-rich (dust=Y) S0 and Es,b galaxies (Graham 2024b, table 2). The long black line denotes galaxies built from major mergers (Graham 2023c, table 1). The steepest (blue) line in the lower-right denotes S galaxies (Graham 2023c, table 1), shown to follow a steep ‘blue sequence’ by Savorgnan et al. (2016) and Davis et al. (2018). The very numerous (in the local Universe) dust-poor S0 galaxies (orange and red squares) with low stellar masses do not follow either of these relations.

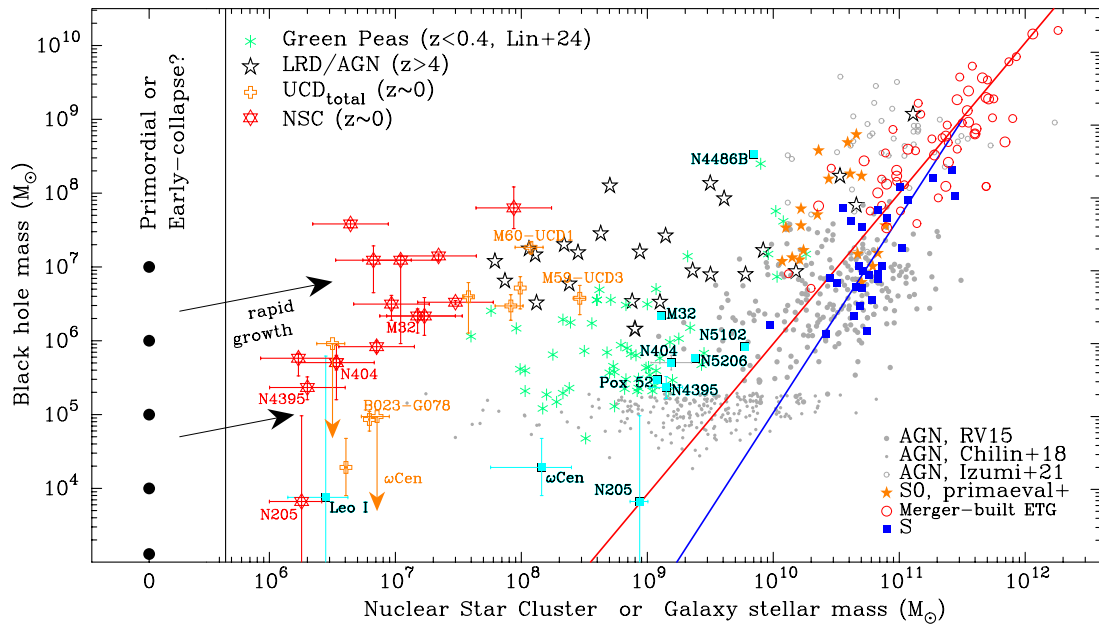


**Figure 3.** Modification of Fig. 2. The quasi-quadratic (black) line denotes galaxies built from major mergers (Graham 2023c, table 1) while the quasi-cubic (blue) line denotes S galaxies (Graham 2023c, table 1), known to follow the steeper ‘blue sequence’ discovered by Savorgnan et al. (2016). The  $z < 0.055$  AGN (larger grey dots) from Reines & Volonteri (2015) have been added; they support the steep quadratic/cubic  $M_{\text{bh}}-M_*$  relations; that is, they are not an offset population. The smaller grey dots are low- $z$  galaxies with AGN hosting suspected intermediate-mass black holes (Chilingarian et al. 2018). The open grey circles are  $z \gtrsim 6$  AGN with dynamical, rather than stellar, galaxy masses (Izumi et al. 2021). Lower-right legend: RV15 = Reines & Volonteri (2015); Chilin+18 = Chilingarian et al. (2018); Izumi+21 = Izumi et al. (2021); ‘Spiral’ = S galaxies with a directly-measured SMBH mass. ‘Merger-built ETG’ = S0, ES, E and BCG with a directly-measured SMBH mass and known to have been built from a major merger; ‘S0, primaeval+’ = dust-poor low mass galaxies with a directly-measured SMBH mass and not known to have experienced a major merger; the + acknowledges that some of these overlap with the S galaxies and as such are likely to be faded S galaxies rather than faded/preserved S0 galaxies that never sufficiently grew to host a spiral pattern.

& Peterson (2006), calibrated to a virial factor  $f = 5.5$  (Onken et al. 2004). Here, these SMBH masses have been reduced by a factor of 3/5.5, which aligns with the calibration used by Graham & Scott (2015).

*JWST* has enabled the detection of AGN in LRDs over a broad range of high redshifts ( $\sim 3-4$  to  $\sim 9-11$ ). Image resolution inhibits our ability to discern multiple components in these LRDs. They may be single-component quasi-spheroidal systems, or maybe they have a denser NSC, or perhaps they are the central region of S0 galaxies in formation, also possibly harbouring an NSC. LRD data from the studies listed below have been included in Figures 1–3, with the *same* total stellar mass plotted in all diagrams.

Another limitation of sorts that may not matter given the broad distribution of LRDs in the diagrams pertains to their adopted stellar mass-to-light ( $M/L$ ) ratios, which have been taken as given in the literature due to the complexities involved in establishing these values. For example, metallicity can affect the fragmentation of gas clouds into stars and, thus, the star’s initial mass function (IMF). The range of stellar ages and internal dust attenuation also impact the adopted stellar  $M/L$  ratio. We additionally note that the mass of the evolved stellar populations in today’s galaxies may have been greater prior to the stellar-to-gas mass conversion arising from stellar winds and supernovae during the galaxy ageing process. Of course, some fraction of this second-generation gas may have turned into new stars.

The LRD data shown here are from (Kokorev et al. 2023, one LRD at  $z = 8.502$ ), (Furtak et al. 2024, one LRD at  $z = 7.045$ ), (Larson et al. 2023, one LRD at  $z = 8.679$ ), (Maiolino et al. 2024, GNZ11 at  $z = 10.603 = \text{GNZ11}$ ), (Übler et al. 2023, one LRD at  $z = 5.55$ ), (Ding et al. 2023, two LRDs at  $z = 6.34$  and  $6.40$ ), (Kocevski et al. 2023, two LRDs at  $z = 5.242$  and  $5.624$ ), (Harikane et al. 2023, 9 LRDs at

$4 < z < 6$  plus one LRD at  $z = 6.936$ ), and (Maiolino et al. 2023, 12 new LRDs at  $4 < z < 7$ ).

### 3. Context Setting and Discussion of Results

#### 3.1. Background Briefing: Life is not linear

For over a decade, it has been understood that a near-linear  $M_{\text{bh}}-M_{*,\text{sph}}$  relation is inadequate to describe ‘ordinary’ galaxies with ‘classical’ (merger built) bulges (as initially explained in Graham 2012); see also (Laor 1998, 2001; Wandel 1999; Salucci et al. 2000). It is now recognised that each galaxy type follows a notably steeper than linear distribution (Graham 2023c), and recognition of galaxy-morphology-specific relations has enabled considerable breakthroughs in our understanding of galaxy evolution. For example, recognition of the galaxy-morphology-dependent  $M_{\text{bh}}-M_{*,\text{sph}}$  relations has led to the identification of two types of S0 galaxies (those known to have low-metallicities and old ages are referred to as primaeval (Conselice et al. 2003; Lisker et al. 2006; Sil’chenko 2013); the other is built from wet major mergers (Graham 2023b)). In the past, these primaeval galaxies may have accreted gas and experienced minor mergers in such a way that they morphed into S galaxies, or a substantial collision may have led them to bypass such a transition and become a second-generation major-merger-built S0 galaxy, which can also be made from S galaxy collisions. Graham (2023c) has suggested that these low-mass, dust-free S0 galaxies are preserved, albeit faded, primaeval galaxies. Ram-pressure stripping of cold gas from these galaxies within the hot X-ray emitting gas clouds/haloes of galaxy groups and clusters can act to preserve them by shutting down star formation. The high velocities of the galaxies in the clusters inhibit mergers of the low-mass galaxies and



prevent this avenue of evolution. The cluster environment effectively ‘pickles’ these galaxies. The bulk of this galaxy type, often referred to as dwarf E (dE) or dwarf ETG (dETG), are known to be nucleated (e.g. Binggeli et al. 1985; Sandage et al. 1985), with even more found using the *Hubble Space Telescope* (e.g. Graham & Guzmán 2003; Côté et al. 2006). As early as Romanishin et al. (1977), some considered these S0 disc galaxies. This has contributed to replacing the Tuning Fork diagram with an evolutionary scheme, dubbed the ‘Triangular’, linking the galaxy types through accretions and mergers (Graham 2023c). The impact of mergers is widespread and wide-scale, from the erosion of NSCs at the centres of galaxies (Bekki & Graham 2010) to a potential ‘merger bias’<sup>u</sup> affecting measurements of the baryonic acoustic oscillations (BAO) used to probe cosmology (Eisenstein et al. 2005; Percival et al. 2007).<sup>v</sup> As we shall see in Section 3.3, these morphology-specific relations are important for understanding the distribution of AGN in the  $M_{\text{bh}}-M_{\star}$  diagram. The distribution of the  $z=0$  primaeval S0 galaxies is also interesting for checking potential connections with the distant LRDs, as done in Section 3.2.

For those new to the evolving field of black hole scaling relations, a quick recap of select relevant developments over the past decade might be helpful. Other readers may wish to jump to the next paragraph. Graham (2012) was the first to point out that the low-mass end of the  $M_{\text{bh}}-M_{\star,\text{sph}}$  relation must be roughly quadratic or steeper to achieve consistency with the  $M_{\text{bh}} \propto \sigma^4-\sigma^5$  and  $M_{\star,\text{sph}} \propto \sigma^2$  relations, and a super-quadratic<sup>w</sup>  $M_{\text{bh}}-M_{\text{gal,dyn}}$  relation was observed among galaxies with Sérsic, as opposed to core-Sérsic<sup>x</sup>, light profiles. That work used the dynamical galaxy masses,  $M_{\text{gal,dyn}}$ , from Häring & Rix (2004). Graham & Scott (2013) and Scott et al. (2013) subsequently measured a super-quadratic  $M_{\text{bh}}-(\text{luminosity}, L_{\text{sph}})$  and  $M_{\text{bh}}-M_{\star,\text{sph}}$  relation for Sérsic galaxies. The state of affairs at that time was reviewed by Graham (2016b), with references to many often forgotten and overlooked papers. Savorgnan et al. (2016) reported an ill-defined super-quadratic  $M_{\text{bh}}-M_{\star,\text{sph}}$  relation for S galaxies with a slope between 2 and 3 and measured  $M_{\text{bh}} \propto M_{\star,\text{sph}}^{1.48 \pm 0.20}$  for those ETGs with a Sérsic light profile. Davis et al. (2019) refined the relation for the S galaxies, finding  $M_{\text{bh}} \propto M_{\star,\text{sph}}^{2.44 \pm 0.30}$ , while separating the S0 and E galaxies, Sahu et al. (2019) observed parallel but offset relations with slopes  $\approx 1.9 \pm 0.2$ . Using colour-dependent (stellar mass)-to-light ratios and updated image decompositions for seven galaxies (Graham & Sahu 2023b), Graham & Sahu (2023a, their table 2 and figure 8) reported shallower slopes of  $\sim 1.6 \pm 0.2$  for the  $M_{\text{bh}}-M_{\star,\text{sph}}$  relations of the S0 and E galaxies, and  $2.25 \pm 0.39$  for the S galaxies. Splitting the S0 galaxy sample (Graham 2023b) into what was effectively those built from a wet major merger (typically dust-rich, disturbed morphologies, previously identified as mergers in the literature) and those that appear primaeval (dust-poor, low stellar mass, typically old) and separating the BCG (typically built from multiple mergers) from the ordinary E galaxies, Graham (2023c) and Graham (2024b) presented

<sup>u</sup>‘Merger bias’ is a term introduced here to capture how luminous red galaxies (LRGs) merge and thus reduce in number over time when building BCGs in clusters that trace the BAO boundary walls. At the same time, new LRGs, such as dust-rich S0 galaxies, form from lower-mass mergers in groups (with lower velocity dispersions congenial to mergers) that are initially out of clusters but fall towards them over time (Sawangwit et al. 2011; Angulo et al. 2014; Kim et al. 2015). Such spatial evolution in the distribution of LRGs due to mergers might introduce an evolving bias with redshift that skews BAO ‘standard ruler’ measurements, complicating claims about an evolving dark energy equation of state.

<sup>v</sup>The abundance of AGN with redshift offers another probe of the time evolution of the equation of state parameter (Lamastra et al. 2012).

<sup>w</sup>The term ‘super-quadratic’ is used to refer to a log-linear relation with a slope greater than 2 but not as high as 3.

<sup>x</sup>Massive galaxies built from dry (gas-poor) major merger events have depleted cores well-described by the core-Sérsic model (Graham et al. 2003). Bulges built from wet mergers have Sérsic light profiles and often additional nuclear components (Balcells et al. 2003; Graham & Guzmán 2003; Balcells et al. 2007).

updated  $M_{\text{bh}}-M_{\star,\text{sph}}$  and  $M_{\text{bh}}-M_{\star,\text{gal}}$  relations that are again quadratic or super-quadratic for the two S0, E and BCG galaxy types.<sup>y</sup> This breakthrough solved why the S galaxies had appeared as a bridging population between the full samples of S0 and E galaxies in previous  $M_{\text{bh}}-M_{\star,\text{sph}}$  diagrams (Sahu et al. 2019; Graham & Sahu 2023a). The low-mass dust-poor S0 galaxies are regarded as primaeval because they did not evolve into a new galaxy type and tend to reside to the left of the lines shown in Figures 2 and 3.

It may be helpful to note that a detected offset in an  $M_{\star}-\sigma$  diagram between ETGs with and without directly measured black hole masses, which had potentially implied a bias in the  $M_{\text{bh}}-M_{\star}$  relations derived from galaxies with directly measured black hole masses (Shankar et al. 2016), was entirely due to a mismatch in the stellar light-to-mass conversion between the data sets (Sahu et al. 2023). The  $M_{\text{bh}}-M_{\star}$  relations should be applied as is to galaxies without directly-measured black hole masses; one simply needs to ensure that the stellar masses of their sample were derived consistently with that used to establish the scaling relation.<sup>z</sup>

Fig. 1 shows that NSCs and the dense inner components of UCDS have stellar masses 2 to 3 orders of magnitude smaller than local galaxies of the same black hole mass. Curiously, they roughly follow a distribution with a similar slope. While new NSC and UCD data has been included (see Section 2.1.2), the line shown on the left-hand side of Fig. 1 has been taken from Graham (2020) and is essentially that first reported by Graham (2016a). A future paper will present an updated analysis of this relation. The main objective here is to see how the LRDs compare. In Figures 2–3, the total (NSC + envelope) stellar mass of the UCDS is plotted.

### 3.1.1. The bridging population of ES galaxies

Although not highlighted in the figures, we mention the local massive ‘compact galaxies’ (Zwicky & Kowal 1968; Zwicky & Zwicky 1971) given that some works (e.g. Trujillo et al. 2014; Saulder et al. 2015) are renaming these ‘relic galaxies’ due to their similarity to the compact massive galaxies at  $z \sim 2.5 \pm 1$ , aka red nuggets (Daddi et al. 2005; van Dokkum et al. 2008; Damjanov et al. 2011). They have sizes and masses comparable to the bulges of today’s dust-rich S0 galaxies (Graham 2013; Hon et al. 2023) and encapsulate the ES,b galaxies shown in Graham & Sahu (2023b). Here, the four ES,b galaxies (with *Spitzer Space Telescope* imaging and multicomponent decompositions) have been grouped with the dust-rich S0 galaxies.

For readers unfamiliar with the ES galaxy type introduced by (Martha) Liller (1966), they have embedded, intermediate-scale stellar discs that do not dominate the light at large radii (e.g. Nieto et al. 1988; Arnold et al. 2011; Graham et al. 2012; Buta et al. 2015; Savorgnan & Graham 2016b).<sup>aa</sup> As noted in the Introduction of Graham (2024b), this population is similar, but not equal, to the ‘discy ellipticals’ presented by Nieto et al. (1988), Nieto & Bender (1989), and Scorza & Bender (1995). The ES,b galaxies are compact and akin to bulges, while the ES,e subtype are extended and more like E galaxies (Graham & Sahu 2023b). Residing near the top of the wet-major-merger-built S0 galaxy sequence, the ES,b galaxies may be relic mergers. This would then rule them out as larger evolved counterparts of LRDs in the sense of evolution by simple gas accretion. Red nuggets might, however,

<sup>y</sup>The offset of the BCGs is also apparent in the  $M_{\text{bh}}-M_{\star,\text{gal}}$  diagram and is explained in Graham & Sahu (2023b) and quantified in Graham (2024b).

<sup>z</sup>The  $M_{\text{bh}}-M_{\star}$  relations for the galaxies shown here were obtained using a diet-Salpeter IMF (Bell & de Jong 2001). Conversion factors for other IMFs are available in Graham & Sahu (2024).

<sup>aa</sup>Buta et al. (2015) labelled many ES galaxies S0<sup>-</sup>sp/E5-E7. However, (E1-E4)-looking galaxies can be ES galaxies with either face-on or edge-on discs at interior radii.

be morphed descendants of LRDs in the sense of a (major merger)-induced ‘punctuated equilibrium’ event, i.e. collision, that transformed the primaevial discs into these more bulge-dominated galaxies at high redshift.

Although multiple stellar populations were not detected in the local ES,b galaxies Mrk 1216, NGC 1271, or NGC 1277 (Walsh et al. 2015; Yıldırım et al. 2015) — which might be odd given their bulge/disc nature if not for their old ages — Rusli et al. (2011) tentatively report different populations in NGC 1332 (dust=y) and Poci et al. (2019) measure differences within NGC 3115 (dust=Y), which is reported to have a spatially offset AGN due to a past merger (Menezes et al. 2014). The ES,b galaxy NGC 1277 became well known after it was thought to have an over-massive black hole giving an  $M_{\text{bh}}/M_{*,\text{sph}}$  ratio of 0.59 (van den Bosch et al. 2012). However, the black hole mass was overestimated by an order of magnitude and the spheroid mass underestimated by the same amount (Graham et al. 2016a). As such, NGC 1277 is not considered an analogue of an LRD with a particularly high  $M_{\text{bh}}/M_{*,\text{sph}}$  ratio. The large, extended ES,e galaxies highlighted in the figures have similar  $B/T$  ratios to the ES,b galaxies. They are built by (perhaps lower redshift) mergers (Graham 2024b, and references therein). However, they have notably lower  $M_{\text{bh}}/M_{*,\text{sph}}$  ratios and lower stellar densities within their spheroid’s half-light radii (Graham & Sahu 2023b, their table 1). With that observation, we have finished our discussion of the poorly-known ES galaxy types, which are yet to come into their own.

### 3.2. LRDs with AGN

Many ideas exist about how SMBHs established themselves early in the Universe (e.g. Inayoshi et al. 2020, and references therein). At first glance, the high SMBH masses of the LRDs at high- $z$  may seem to favour heavy BH seeds over light seeds, and one might even speculate that they could be primordial, contributing to dark matter (e.g. Argyres et al. 1998; Bean & Magueijo 2002; Dolgov & Postnov 2017). The direct collapse of gas clouds (Doroshkevich et al. 1967; Umemura et al. 1993) and self-gravitating pre-galactic gas disks (Begelman et al. 2006; Spaans & Silk 2006) has been proposed for the production of more massive seed black holes. At the same time, there can still be a contribution from light BH seeds, including those built from the cascading collision of stars in dense clusters at the nuclei of haloes (Portegies Zwart & McMillan 2002; Omukai et al. 2008; Das et al. 2021). In the presence of substantial gas, dynamical friction will help feed these cluster stars inward (Omukai et al. 2008; Devecchi & Volonteri 2009; Davies et al. 2011). This will contribute to the partial demise of the clusters and the growth of the massive black holes. There is also near-Eddington (Wolf et al. 2024) and super-Eddington accretion (Volonteri & Rees 2005; Alexander & Natarajan 2014) onto these high- $z$  BHs, perhaps formed from Pop III stars (Ryu et al. 2016; Banik et al. 2019; Tan et al. 2024). Indeed, Suh et al. (2024) recently reported on LID-568, an SMBH at  $z \approx 4$ , accreting at 40 times the Eddington limit. A combination of light and heavy black holes may have seeded the LRDs.

There may be clues at low- $z$  as to the evolution of LRDs. The cE galaxies at  $z \sim 0$  are considered former disc galaxies stripped of many of their stars (e.g. Zinnecker et al. 1988; Freeman 1993; Khoperskov et al. 2023). At the same time, some rare isolated cEs may have simply never ‘grown up’, unless they are all runaway systems stripped and then ejected from galaxy groups or clusters (Chilingarian & Zolotukhin 2015). As illustrated in Graham & Sahu (2023b, their figure 6), stripping of stars can produce galaxies with  $M_{\text{bh}}/M_{*,\text{sph}} \approx 0.05$  (e.g. NGC 4486B around M87, or NGC 4342). The more extreme version of stripping, referred to as ‘threshing’ (e.g. Bekki & Freeman 2003; Ideta & Makino 2004; Chilingarian & Mamon 2008; Pfeffer & Baumgardt

2013), is thought to produce UCDs. SDSS J124155.33+114003.7, for which we do not have a black hole mass, may represent a halfway point between cEs and UCDs (Chilingarian & Mamon 2008). Threshing can pare a galaxy back to  $M_{\text{bh}}/M_{*,\text{sph}} \sim 0.1$  (e.g. UCD1 around M60) or perhaps even  $\sim 1$  if just the NSC remains.

It can be seen that LRDs are not quite similar to NSCs for which Graham & Spitler (2009) quantified their  $M_{\text{bh}}/M_*$  ratios. Figures 2–3 reveal that the LRDs tend to have smaller  $M_{\text{bh}}/M_*$  ratios, with some matching that of UCDs and likely revealing that we are witnessing more than just a dense (single-component) star cluster; that is, observing a more extended galaxy.<sup>ab</sup> Through the LRDs, we are presumably witnessing the reverse of a stellar stripping process, in which the black hole mass is already in place or quickly forms before the bulk of a galaxy’s stellar mass builds around it.

Given that the stripping process should preferentially remove the dark matter (thought to be dominant at larger, and thus less bound, radii)<sup>ac</sup>, a key difference between local UCDs formed via stripping and relic LRDs may be their dark matter fraction. The lack of dark matter in UCD galaxies (e.g. Hilker et al. 2007; Chilingarian et al. 2011; Frank et al. 2011) would seem to rule out the notion of them being compact galaxies formed in dark matter haloes, i.e. LRDs, as opposed to tidally-stripped galaxies. One may also speculate that all of today’s UCDs should contain a massive black hole if all high- $z$  LRDs did. It is not, however, established that all local UCDs contain a massive black hole, nor if all nucleated dwarf S0 galaxies — the likely pre-stripped progenitors of UCDs — do. This may be an issue of spatial resolution rather than absence. Furthermore, the *first* LRDs to form are perhaps unlikely to be today’s UCDs, as these early LRDs probably resided in larger over-densities that eventually became today’s massive ETGs. However, the LRDs that formed later in the Universe, in smaller haloes, might be the ancestors of today’s UCDs (nuclei of threshed low-mass disc galaxies that were once LRDs). As such, not all UCDs should be expected to have a purely old stellar population.

In passing, it is noted that the stellar population of LRDs (and red nuggets) would have initially been blue due to hot, massive stars, just as the stars in the discs of today’s low-mass disc-dominated S0 galaxies would have been more<sup>ad</sup> blue in the past when they were younger. Ideally, future work will reveal further connections between LRDs and green peas (Cardamone et al. 2009; Lin et al. 2024a), blue dwarf ETGs (Cairós et al. 2001, 2003; Driver et al. 2007; Cameron et al. 2009; Moffett et al. 2016, 2019), and luminous blue compact galaxies (Guzmán et al. 2003; Shi et al. 2005; Bergvall et al. 2006; Pérez-Gallego et al. 2011).

The notion that most S galaxies reside below the original near-linear  $M_{\text{bh}}-M_*$  relation because they have pseudobulges and their black hole mass is yet to ‘catch up’ to their stellar mass seems quite untenable given the high  $M_{\text{bh}}/M_*$  ratios of the distant LRDs that evolved into today’s galaxies. Instead, it appears that evolution has proceeded with the stellar mass playing catch up to the black hole mass to bring the distant/younger galaxies in line with the local  $M_{\text{bh}}-M_*$  relations. Indeed, the secular formation of pseudobulges would not make S galaxies reside below the distribution of ETGs in the  $M_{\text{bh}}-M_{*,\text{gal}}$  diagram. The location of the S galaxies in the  $M_{\text{bh}}-M_*$  diagrams is instead explained in terms

<sup>ab</sup>The LRD with the exceptionally high mass is SDSS J2236+0032 (Ding et al. 2023). In Fig. 2, it resides next to the ES,b galaxy NGC 1332 and the dust-rich S0 galaxy NGC 6861, suggesting it is more akin to a ‘red nugget’ than an LRD, as does its half-light radius of  $0.7 \pm 0.1$  kpc in the F356W filter (Ding et al. 2023).

<sup>ac</sup>Proponents of modified gravity offer an alternate view (Milgrom 1983; Moffat 2006; De Felice & Tsujikawa 2010; Famaey & McGaugh 2012; de Martino et al. 2020, their section 5.1).

<sup>ad</sup>Due to low metallicity, dwarf S0 galaxies are at the blue/green end of the ‘red sequence’ (Baum 1959; de Vaucouleurs 1961; de Vaucouleurs & de Vaucouleurs 1972; Graham 2024a, and references therein).



of disc/bulge growth through accretion and minor (non-disc-destroying) mergers (Graham 2023c). Is such growth ceased long ago, one will be left with a primaeval galaxy today. Using the total stellar mass of the LRDs causes some to overlap with the spheroidal/bulge component of local S and S0 galaxies built from major wet mergers in the  $M_{\text{bh}}-M_{*,\text{sph}}$  diagram (Fig. 1). However, the total stellar mass of LRDs falls short of matching the total stellar masses of these same galaxies in the  $M_{\text{bh}}-M_{*,\text{gal}}$  diagram (Fig. 2). The simple conclusion is that LRDs have discs, and the assignment of all their stellar mass to a spheroidal component, as done in Fig. 1, is incorrect. That is, by using both the  $M_{\text{bh}}-M_{*,\text{sph}}$  and  $M_{\text{bh}}-M_{*,\text{gal}}$  diagrams, together with the galaxy-morphology-specific relations, we deduce that comparison of LRDs with local galaxies in the  $M_{\text{bh}}-M_{*,\text{sph}}$  diagram is most likely not appropriate unless galaxy structural engineers deconstruct the images of the LRDs and extract their bulge component. Until then, the  $M_{\text{bh}}-M_{*,\text{gal}}$  diagram should be preferred.

Finally, we are open to the possibility that whether UCDs and some LRDs are structurally equivalent could be a case of ‘naïve realism’ based on ‘the illusion of information adequacy’ (Gehlbach et al. 2024), stemming from their congruent location in the  $M_{\text{bh}}-M_{*,\text{gal}}$  diagram. Additional information may suggest that their overlap in SMBH and stellar masses is a mere coincidence. In this regard, size information of LRDs and age estimation of UCD galaxies (e.g. Chilingarian et al. 2008) should be valuable. At least some UCDs are measured to be reasonably old, such as the Sombrero galaxy’s SUCD1 at  $12.6 \pm 0.9$  Gyr (Hau et al. 2009) and M60-UCD1 with a formal age of  $14.5 \pm 0.5$  Gyr (Seth et al. 2014), older than the Universe. However, the Virgo cluster’s VUCD3 is reported to have an age of just 11 Gyr with a 9.6-Gyr-old inner component, while M59cO has an age of 11.5 Gyr but with an inner component of just 5.5 Gyr (Ahn et al. 2017). This may reflect the ability of star clusters to rejuvenate themselves, at least those residing at the bottom of a galaxy’s gravitational potential well, or a late-time creation for some. Detecting elongated LRDs with light profiles having Sérsic indices  $n \lesssim 1$  would suggest they are disc structures.

### 3.3. Additional AGN: toeing the line

As noted in the Introduction, the steep quadratic nature of the  $M_{\text{bh}}-M_{*,\text{sph}}$  relations for ETGs built from major mergers naturally place bright QSOs (e.g. Wang et al. 2010; Bongiorno et al. 2014; Wang et al. 2016; Shao et al. 2017; Decarli et al. 2018; Venemans et al. 2016) above the original near-linear relation. At the same time, the super-quadratic  $M_{\text{bh}}-M_{*,\text{sph}}$  (and cubic  $M_{\text{bh}}-M_{*,\text{gal}}$ ) relation for S galaxies naturally places faint Seyfert galaxies below the original near-linear relation (Reines & Volonteri 2015). Bridging these extremes are the low-luminosity QSOs and regular AGN of intermediate-luminosity (Willott et al. 2015, 2017; Izumi et al. 2018) that overlap with the original near-linear  $M_{\text{bh}}-M_{*}$  relation. Izumi et al. (2021) reported how the less luminous QSOs beyond  $z \sim 6$  had  $M_{\text{bh}}/M_{*}$  ratios more in line with the original near-linear  $M_{\text{bh}}-M_{*}$  relation. Rather than talking in terms of differing and disjoint populations of AGN with over- or under-massive black holes, it makes more sense to recognise that the original proposition of a linear  $M_{\text{bh}}-M_{*}$  scaling relation requires adjusting and that a steeper scaling relation unifies many galaxies.

The lack of morphological information among AGN samples has hampered past understanding of galaxy speciation. However, as briefly noted before, one slight mystery has now been resolved. In Fig. 1, and the  $M_{\text{bh}}-M_{*,\text{sph}}$  diagram presented in Graham & Scott (2015), some of the AGN were seen to reside to the right of the sample of galaxies with predominantly inactive black holes with directly measured masses. This is evident at  $M_{\text{bh}} \approx 10^7 M_{\odot}$ . From the  $M_{\text{bh}}-M_{*,\text{gal}}$  diagram (Fig. 2), it

is apparent that these AGN are probably S galaxies. It is likely that the published  $B/T$  ratios for these AGN, which were typically greater than 0.5-0.6, were too high. S galaxies tend to have  $B/T < 0.1-0.2$  (Graham & Worley 2008; Davis et al. 2019).

Given the location of the AGN with  $M_{\text{bh}} \lesssim 10^6 M_{\odot}$  in Fig. 1 and Fig. 2, they appear to be hosted by S galaxies and primaeval S0 galaxies. Again, the term primaeval is used to imply a first-generation galaxy type not altered by substantial accretion or major mergers. These AGN are consistent with the steep morphology-specific  $M_{\text{bh}}-M_{*}$  scaling relations, even though they were not used to define them.

A simplified variant of Fig. 2 is presented in Fig. 3, such that the local sample of galaxies with directly measured SMBH masses is now separated into just three types. There are those previously identified as primaeval; they are the low-mass, dust-poor S0 disc galaxies that tend to have an old, metal-poor stellar population. Second are the disc galaxies with a spiral pattern, which tend to have ongoing star formation.<sup>ac</sup> Then there are the galaxies built from major mergers, such as the (often dust-rich) S0 galaxies built from a wet major merger, the E galaxies built from a dry major merger, and the BCG typically built from more than one major merger. This subdivision offers an alternative view of how the local AGN mesh with, rather than deviate from, galaxies with varying formation histories.

Fig. 3 also displays new samples of AGN. The AGN with estimated black hole masses from Reines & Volonteri (2015) and Chilingarian et al. (2018) are included, as are the AGN at  $z \gtrsim 6$  from Izumi et al. (2021). However, only dynamical, rather than stellar, galaxy masses are published for this final sample. Therefore, a (not overly prominent) small grey circle is used to show those systems in Fig. 3. While Izumi et al. (2021, their figure 13) reported that many of these systems have overmassive black holes (by up to a factor of  $\sim 10$ ) relative to the old near-linear  $M_{\text{bh}}-M_{*}$  relation, the bulk of them are not outliers relative to the steeper galaxy-morphology-dependent  $M_{\text{bh}}-M_{*}$  relation for merger-built S0 galaxies, a point made by Graham (2023b), see also Graham & Sahu (2023a). Just 3 to 5 of these AGN from Izumi et al. (2021) have  $M_{\text{bh}}/M_{\text{dyn}}$  ratios that are a factor of (only) 2 to 3 times higher than the distribution seen for local systems with directly measured SMBH masses. This is reconcilable with the sample selection bias of the most luminous QSOs at high- $z$  and the greater inaccuracy of indirect measures of black hole mass in AGN. The subset of luminous  $z \gtrsim 6$  AGN from Izumi et al. (2021) shown in Fig. 3 is likely to be wet-merger-built S0 galaxies.

At  $M_{*,\text{gal}} > 10^{10} M_{\odot}$ , in Fig. 3, the overlap of low- $z$  AGN with the  $z \approx 0$  sample of SMBHs with directly measured masses reveals that these AGN are predominantly S galaxies or merger-built S0 galaxies. These AGN are not an offset population from ordinary galaxies with predominantly inactive SMBHs.

Knowledge of galaxy-morphology-specific black hole scaling relations and offsets from these enables an improved means for deriving the virial factor(s) for converting AGN virial products into black hole masses (Peterson 1993; Onken et al. 2004; Bentz et al. 2009). To date, these have mainly been obtained with little attention to galaxy morphology. A better approach will involve matching AGN virial products with directly measured black hole masses from galaxies of the same morphological type (Graham et al. 2024, in preparation). It can already be seen in the data of Bentz & Manne-Nicholas (2018, their figure 5) that the reverberation-mapped AGN follow a steep  $M_{\text{bh}}-M_{*,\text{sph}}$  distribution well-matched by the super-quadratic relation quantified by Scott et al. (2013, their figure 3) for galaxies without depleted stellar cores, i.e. those not built from a dry major merger. Similarly, the AGN data

<sup>ac</sup> Arguably, gas-stripped and faded S galaxies, which are now S0 galaxies, belong to this category.

of Bentz & Manne-Nicholas (2018, their figure 6) display a steep trend similar to that of Savorgnan et al. (2016) for S galaxies. This yet-to-be-applied approach will avoid a bias such that the reverberation-mapped AGN sample may be skewed toward a distribution of galaxy type, such as S and dust-rich S0 galaxies, that differs from the bulk of the sample with directly measured black hole masses to which it is compared. Similarly, AGN sample selection of certain galaxy types and not others, for example, S and/or dust-rich S0 but not primaeval dust-poor S0 galaxies or ‘red and dead’ E galaxies, may also explain the tight AGN relations reported by Bennert et al. (2021). The location of the LRDs and other AGN in Figures 1–3 will be refined once improved virial factors are established by applying the galaxy-morphology-dependent scaling relations (Graham 2023c).

#### 4. Summary

This paper added high- $z$  LRDs and low- $z$  AGN to  $M_{\text{bh}}-M_{\star}$  diagrams that, for the first time, included UCDs and NSCs. Our diagrams also identified an expanded set of galaxy morphologies. In addition, galaxy-morphology-specific  $M_{\text{bh}}-M_{\star}$  relations were shown rather than a single near-linear relation for low- $z$  galaxies with AGN and a separate single near-linear relation for inactive galaxies. Unlike previous  $M_{\text{bh}}-M_{\star}$  relations based on various fractions of ETGs and LTGs or all of the different ETGs combined, these morphology-specific relations avoid sample selection bias from mixing different galaxy types that follow distinct  $M_{\text{bh}}-M_{\star}$  relations.

The LRDs were shown to span the  $M_{\text{bh}}-M_{\star, \text{gal}}$  diagram from UCDs to previously recognised primaeval galaxies.

We demonstrated that several samples of low- $z$  AGN, including candidate intermediate-mass black holes (Graham & Scott 2015; Chilingarian et al. 2018), broadly overlap with the steep, non-linear, galaxy-morphology-dependent  $M_{\text{bh}}-M_{\star}$  relations. This suggests that using galaxy samples with similar morphology may be worthwhile in re-determining the virial factor used to estimate black hole masses in AGN and LRDs. Furthermore, adjustments to high  $z$  QSO and LRD black hole masses will impact expectations for black hole seed masses and early accretion rates.

#### Acknowledgements

This paper is dedicated to Alexander Bolton Graham (1933-2024), who adopted AWG many years ago and patiently listened (as a frequent hospital patient in 2020-2024) to unpublished developments in galaxy/black hole research.

This research has used the SAO/NASA Astrophysics Data System (ADS) bibliographic services.

#### References

- Ahn C. P., et al., 2017, *ApJ*, **839**, 72  
 Akins H. B., et al., 2024, *arXiv e-prints*, p. [arXiv:2406.10341](https://arxiv.org/abs/2406.10341)  
 Alexander T., Natarajan P., 2014, *Science*, **345**, 1330  
 Amaro-Seoane P., et al., 2023, *Living Reviews in Relativity*, **26**, 2  
 Ananna T. T., Bogdán Á., Kovács O. E., Natarajan P., Hickox R. C., 2024, *ApJ*, **969**, L18  
 Angulo R. E., White S. D. M., Springel V., Henriques B., 2014, *MNRAS*, **442**, 2131  
 Argyres P. C., Dimopoulos S., March-Russell J., 1998, *Physics Letters B*, **441**, 96  
 Arnold J. A., Romanowsky A. J., Brodie J. P., Chomiuk L., Spitler L. R., Strader J., Benson A. J., Forbes D. A., 2011, *ApJ*, **736**, L26  
 Babak S., et al., 2017, *Phys. Rev. D*, **95**, 103012  
 Balcells M., Graham A. W., Domínguez-Palmero L., Peletier R. F., 2003, *ApJ*, **582**, L79  
 Balcells M., Graham A. W., Peletier R. F., 2007, *ApJ*, **665**, 1084  
 Banik N., Tan J. C., Monaco P., 2019, *MNRAS*, **483**, 3592  
 Barro G., et al., 2024, *ApJ*, **963**, 128  
 Baum W. A., 1959, *PASP*, **71**, 106  
 Bean R., Magueijo J., 2002, *Phys. Rev. D*, **66**, 063505  
 Begelman M. C., Blandford R. D., Rees M. J., 1980, *Nature*, **287**, 307  
 Begelman M. C., Volonteri M., Rees M. J., 2006, *MNRAS*, **370**, 289  
 Bekki K., Freeman K. C., 2003, *MNRAS*, **346**, L11  
 Bekki K., Graham A. W., 2010, *ApJ*, **714**, L313  
 Bekki K., Couch W. J., Drinkwater M. J., 2001, *ApJ*, **552**, L105  
 Bell E. F., de Jong R. S., 2001, *ApJ*, **550**, 212  
 Bennert V. N., Auger M. W., Treu T., Woo J.-H., Malkan M. A., 2011, *ApJ*, **742**, 107  
 Bennert V. N., et al., 2021, *ApJ*, **921**, 36  
 Bentz M. C., Manne-Nicholas E., 2018, *ApJ*, **864**, 146  
 Bentz M. C., Peterson B. M., Pogge R. W., Vestergaard M., 2009, *ApJ*, **694**, L166  
 Bergvall N., Zackrisson E., Andersson B. G., Arnberg D., Masegosa J., Östlin G., 2006, *A&A*, **448**, 513  
 Binggeli B., Sandage A., Tammann G. A., 1985, *AJ*, **90**, 1681  
 Bogdán Á., et al., 2024, *Nature Astronomy*, **8**, 126  
 Bongiorno A., et al., 2014, *MNRAS*, **443**, 2077  
 Brodie J. P., Romanowsky A. J., Strader J., Forbes D. A., 2011, *AJ*, **142**, 199  
 Brum C., et al., 2019, *MNRAS*, **486**, 691  
 Bunker A. J., et al., 2023, *A&A*, **677**, A88  
 Busch G., et al., 2014, *A&A*, **561**, A140  
 Buta R. J., et al., 2015, *ApJS*, **217**, 32  
 Cairós L. M., Vílchez J. M., González Pérez J. N., Iglesias-Páramo J., Caon N., 2001, *ApJS*, **133**, 321  
 Cairós L. M., Caon N., Papaderos P., Noeske K., Vílchez J. M., García Lorenzo B., Muñoz-Tuñón C., 2003, *ApJ*, **593**, 312  
 Cameron E., Driver S. P., Graham A. W., Liske J., 2009, *ApJ*, **699**, 105  
 Cappellari M., et al., 2011, *MNRAS*, **416**, 1680  
 Cardamone C., et al., 2009, *MNRAS*, **399**, 1191  
 Chilingarian I. V., Mamon G. A., 2008, *MNRAS*, **385**, L83  
 Chilingarian I., Zolotukhin I., 2015, *Science*, **348**, 418  
 Chilingarian I. V., Cayatte V., Bergond G., 2008, *MNRAS*, **390**, 906  
 Chilingarian I. V., Mieske S., Hilker M., Infante L., 2011, *MNRAS*, **412**, 1627  
 Chilingarian I. V., Katkov I. Y., Zolotukhin I. Y., Grishin K. A., Beletsky Y., Boutsia K., Osip D. J., 2018, *ApJ*, **863**, 1  
 Chomiuk L., Strader J., Brodie J. P., 2008, *AJ*, **136**, 234  
 Ciambur B. C., Graham A. W., 2016, *MNRAS*, **459**, 1276  
 Conselice C. J., Gallagher John S. I., Wyse R. F. G., 2003, *AJ*, **125**, 66  
 Côté P., et al., 2006, *ApJS*, **165**, 57  
 D’Onghia E., Vogelsberger M., Hernquist L., 2013, *ApJ*, **766**, 34  
 D’Souza R., Rix H.-W., 2013, *MNRAS*, **429**, 1887  
 Daddi E., et al., 2005, *ApJ*, **626**, 680  
 Damjanov I., et al., 2011, *ApJ*, **739**, L44  
 Das A., Schleicher D. R. G., Basu S., Boekholt T. C. N., 2021, *MNRAS*, **505**, 2186  
 Davies R. D., Lewis B. M., 1973, *MNRAS*, **165**, 231  
 Davies M. B., Miller M. C., Bellovary J. M., 2011, *ApJ*, **740**, L42  
 Davis B. L., Graham A. W., Cameron E., 2018, *ApJ*, **869**, 113  
 Davis B. L., Graham A. W., Cameron E., 2019, *ApJ*, **873**, 85  
 Davis T. A., et al., 2020, *MNRAS*, **496**, 4061  
 De Felice A., Tsujikawa S., 2010, *Living Reviews in Relativity*, **13**, 3  
 Decarli R., et al., 2018, *ApJ*, **854**, 97  
 Devecchi B., Volonteri M., 2009, *ApJ*, **694**, 302  
 Ding X., et al., 2020, *ApJ*, **888**, 37  
 Ding X., et al., 2023, *Nature*, **621**, 51  
 Dolgov A., Postnov K., 2017, *J. Cosmology Astropart. Phys.*, **2017**, 036  
 Doroshkevich A. G., Zel’dovich Y. B., Novikov I. D., 1967, *Soviet Ast.*, **11**, 233  
 Dressler A., 1989, in Osterbrock D. E., Miller J. S., eds, *IAU Symposium Vol. 134, Active Galactic Nuclei*. Kluwer Academic Publishers, Dordrecht, p. 217  
 Dressler A., Richstone D. O., 1988, *ApJ*, **324**, 701  
 Drinkwater M. J., Jones J. B., Gregg M. D., Phillipps S., 2000, *PASA*, **17**, 227

- Drinkwater M. J., Gregg M. D., Hilker M., Bekki K., Couch W. J., Ferguson H. C., Jones J. B., Phillipps S., 2003, *Nature*, **423**, 519
- Driver S. P., Allen P. D., Liske J., Graham A. W., 2007, *ApJ*, **657**, L85
- Dullo B. T., Graham A. W., 2014, *MNRAS*, **444**, 2700
- Eales S. A., et al., 2018, *MNRAS*, **481**, 1183
- Eisenstein D. J., et al., 2005, *ApJ*, **633**, 560
- Elmegreen D. M., Elmegreen B. G., 2017, *ApJ*, **851**, L44
- Evrard A. E., Summers F. J., Davis M., 1994, *ApJ*, **422**, 11
- Fall S. M., Pei Y. C., 1993, *ApJ*, **402**, 479
- Famaey B., McGaugh S. S., 2012, *Living Reviews in Relativity*, **15**, 10
- Forbes D. A., Ferré-Mateu A., Durré M., Brodie J. P., Romanowsky A. J., 2020, *MNRAS*, **497**, 765
- Frank M. J., Hilker M., Mieske S., Baumgardt H., Grebel E. K., Infante L., 2011, *MNRAS*, **414**, L70
- Freeman K. C., 1993, in Smith G. H., Brodie J. P., eds, *Astronomical Society of the Pacific Conference Series Vol. 48, The Globular Cluster-Galaxy Connection*. p. 608
- Furtak L. J., et al., 2024, *Nature*, **628**, 57
- Gair J. R., Babak S., Sesana A., Amaro-Seoane P., Barausse E., Berry C. P. L., Berti E., Sopuerta C., 2017, in *Journal of Physics Conference Series*. IOP. p. 012021 ([arXiv:1704.00009](https://arxiv.org/abs/1704.00009)), doi:10.1088/1742-6596/840/1/012021
- Gehlbach H., Robinson C. D., Fletcher A., 2024, *PLOS ONE*, **19**, 1
- Gerhard O. E., 1981, *MNRAS*, **197**, 179
- Graham A. W., 2004, *ApJ*, **613**, L33
- Graham A. W., 2007, *MNRAS*, **379**, 711
- Graham A. W., 2012, *ApJ*, **746**, 113
- Graham A. W., 2013, in Oswalt T. D., Keel W. C., eds, *Planets, Stars and Stellar Systems. Volume 6: Extragalactic Astronomy and Cosmology*. Springer Science+Business Media, Dordrecht, pp 91–140, doi:10.1007/978-94-007-5609-0\_2
- Graham A. W., 2014, in Seigar M. S., Treuhardt P., eds, *Astronomical Society of the Pacific Conference Series Vol. 480, Structure and Dynamics of Disk Galaxies*. p. 185 ([arXiv:1311.7207](https://arxiv.org/abs/1311.7207)), doi:10.48550/arXiv.1311.7207
- Graham A. W., 2016a, in Meiron Y., Li S., Liu F. K., Spurzem R., eds, *IAU Symposium Vol. 312, Star Clusters and Black Holes in Galaxies across Cosmic Time*. pp 269–273 ([arXiv:1412.5715](https://arxiv.org/abs/1412.5715)), doi:10.1017/S1743921315008017
- Graham A. W., 2016b, in Laurikainen E., Peletier R., Gadotti D., eds, *Astrophysics and Space Science Library Vol. 418, Galactic Bulges*. p. 263 ([arXiv:1501.02937](https://arxiv.org/abs/1501.02937)), doi:10.1007/978-3-319-19378-6\_11
- Graham A. W., 2020, *MNRAS*, **492**, 3263
- Graham A. W., 2023a, *MNRAS*, **518**, 6293
- Graham A. W., 2023b, *MNRAS*, **521**, 1023
- Graham A. W., 2023c, *MNRAS*, **522**, 3588
- Graham A. W., 2024a, *MNRAS*, **531**, 230
- Graham A. W., 2024b, *MNRAS*, **535**, 299
- Graham A. W., Guzmán R., 2003, *AJ*, **125**, 2936
- Graham A. W., Sahu N., 2023a, *MNRAS*, **518**, 2177
- Graham A. W., Sahu N., 2023b, *MNRAS*, **520**, 1975
- Graham A. W., Sahu N., 2024, *MNRAS*, **530**, 3429
- Graham A. W., Scott N., 2013, *ApJ*, **764**, 151
- Graham A. W., Scott N., 2015, *ApJ*, **798**, 54
- Graham A. W., Spitler L. R., 2009, *MNRAS*, **397**, 2148
- Graham A. W., Worley C. C., 2008, *MNRAS*, **388**, 1708
- Graham A. W., Erwin P., Trujillo I., Asensio Ramos A., 2003, *AJ*, **125**, 2951
- Graham A. W., Onken C. A., Athanassoula E., Combes F., 2011, *MNRAS*, **412**, 2211
- Graham A. W., Spitler L. R., Forbes D. A., Lisker T., Moore B., Janz J., 2012, *ApJ*, **750**, 121
- Graham A. W., Durré M., Savorgnan G. A. D., Medling A. M., Batcheldor D., Scott N., Watson B., Marconi A., 2016a, *ApJ*, **819**, 43
- Graham A. W., Ciambur B. C., Savorgnan G. A. D., 2016b, *ApJ*, **831**, 132
- Graham A. W., Jarrett T. H., Cluver M. E., 2024, *MNRAS*, **527**, 10059
- Gu H., Wu X.-B., Wen Y., Ma Q., Guo H., 2024, *MNRAS*, **530**, 3578
- Gualandris A., Merritt D., 2012, *ApJ*, **744**, 74
- Gunn J. E., Gott J. Richard I., 1972, *ApJ*, **176**, 1
- Guzmán R., Östlin G., Kunth D., Bershady M. A., Koo D. C., Pahre M. A., 2003, *ApJ*, **586**, L45
- Haas M., 1998, *A&A*, **337**, L1
- Häberle M., et al., 2024, *Nature*, **631**, 285
- Hargis J. R., Rhode K. L., Strader J., Brodie J. P., 2011, *ApJ*, **738**, 113
- Harikane Y., et al., 2023, *ApJ*, **959**, 39
- Häring N., Rix H.-W., 2004, *ApJ*, **604**, L89
- Harris W. E., Pritchet C. J., McClure R. D., 1995, *ApJ*, **441**, 120
- Hau G. K. T., Spitler L. R., Forbes D. A., Proctor R. N., Strader J., Mendel J. T., Brodie J. P., Harris W. E., 2009, *MNRAS*, **394**, L97
- Hilker M., Infante L., Vieira G., Kissler-Patig M., Richtler T., 1999, *A&S*, **134**, 75
- Hilker M., Baumgardt H., Infante L., Drinkwater M., Evstigneeva E., Gregg M., 2007, *A&A*, **463**, 119
- Hon D. S. H., Graham A. W., Sahu N., 2023, *MNRAS*, **519**, 4651
- Hopp U., Wagner S. J., Richtler T., 1995, *A&A*, **296**, 633
- Hubble E. P., 1926, *ApJ*, **64**, 321
- Hubble E. P., 1936, *Realm of the Nebulae*. New Haven: Yale University Press
- Ideta M., Makino J., 2004, *ApJ*, **616**, L107
- Inayoshi K., Visbal E., Haiman Z., 2020, *ARA&A*, **58**, 27
- Izumi T., et al., 2018, *PASJ*, **70**, 36
- Izumi T., et al., 2021, *ApJ*, **914**, 36
- Jahnke K., Macciò A. V., 2011, *ApJ*, **734**, 92
- Jeans J. H., 1919, *Problems of cosmogony and stellar dynamics*. Cambridge Univ. Press, Cambridge
- Jeans J. H., 1928, *Astronomy and cosmogony*. Cambridge: Cambridge University Press
- Jiang Y.-F., Greene J. E., Ho L. C., 2011, *ApJ*, **737**, L45
- Jiang N., Ho L. C., Dong X.-B., Yang H., Wang J., 2013, *ApJ*, **770**, 3
- Julian W. H., Toomre A., 1966, *ApJ*, **146**, 810
- Juodžbalis I., et al., 2024, *MNRAS*, **535**, 853
- Khoperskov A. V., Khrapov S. S., Sirotnin D. S., 2023, *Galaxies*, **12**, 1
- Kim J., Park C., L'Huillier B., Hong S. E., 2015, *Journal of Korean Astronomical Society*, **48**, 213
- Kocevski D. D., et al., 2023, *ApJ*, **954**, L4
- Kokorev V., et al., 2023, *ApJ*, **957**, L7
- Kormendy J., Richstone D., 1995, *ARA&A*, **33**, 581
- Krajnović D., et al., 2015, *MNRAS*, **452**, 2
- Lamastra A., Menci N., Fiore F., di Porto C., Amendola L., 2012, *MNRAS*, **420**, 2429
- Lane J. M. M., Bovy J., Mackereth J. T., 2023, *MNRAS*, **526**, 1209
- Langeroodi D., Hjorth J., 2023, *ApJ*, **957**, L27
- Laor A., 1998, *ApJ*, **505**, L83
- Laor A., 2001, *ApJ*, **553**, 677
- Larson R. L., et al., 2023, *ApJ*, **953**, L29
- Leung G. C. K., et al., 2024, *arXiv e-prints*, p. [arXiv:2411.12005](https://arxiv.org/abs/2411.12005)
- Liller M. H., 1966, *ApJ*, **146**, 28
- Limberg G., 2024, *arXiv e-prints*, p. [arXiv:2411.11251](https://arxiv.org/abs/2411.11251)
- Lin R., et al., 2024a, *arXiv e-prints*, p. [arXiv:2412.08396](https://arxiv.org/abs/2412.08396)
- Lin R., et al., 2024b, *Science China Physics, Mechanics, and Astronomy*, **67**, 109811
- Lisker T., Glatt K., Westera P., Grebel E. K., 2006, *AJ*, **132**, 2432
- Lyubenova M., et al., 2013, *MNRAS*, **431**, 3364
- Madrid J. P., et al., 2010, *ApJ*, **722**, 1707
- Magorrian J., et al., 1998, *AJ*, **115**, 2285
- Maiolino R., et al., 2023, *arXiv e-prints*, p. [arXiv:2308.01230](https://arxiv.org/abs/2308.01230)
- Maiolino R., et al., 2024, *Nature*, **627**, 59
- Mapelli M., Ripamonti E., Vecchio A., Graham A. W., Gualandris A., 2012, *A&A*, **542**, A102
- Marleau F. R., et al., 2006, *ApJ*, **646**, 929
- Martig M., Bournaud F., Teyssier R., Dekel A., 2009, *ApJ*, **707**, 250
- Mateo M., Olszewski E. W., Walker M. G., 2008, *ApJ*, **675**, 201
- Mathur S., Fields D., Peterson B. M., Grupe D., 2012, *ApJ*, **754**, 146
- Matthee J., et al., 2024, *ApJ*, **963**, 129
- Menezes R. B., Steiner J. E., Ricci T. V., 2014, *ApJ*, **796**, L13
- Milgrom M., 1983, *ApJ*, **270**, 384
- Moffat J. W., 2006, *J. Cosmology Astropart. Phys.*, **2006**, 004
- Moffett A. J., et al., 2016, *MNRAS*, **457**, 1308
- Moffett A. J., et al., 2019, *MNRAS*, **489**, 2830
- Molaeinezhad A., et al., 2019, *MNRAS*, **488**, 1012



- Mowla L., Iyer K., Asada Y., 2024, *Nature*, 636, 332
- Negroponte J., White S. D. M., 1983, *MNRAS*, 205, 1009
- Nguyen D. D., et al., 2018, *ApJ*, 858, 118
- Nguyen D. D., et al., 2019, *ApJ*, 872, 104
- Nguyen D. D., et al., 2022, *MNRAS*, 509, 2920
- Nieto J. L., Bender R., 1989, *A&A*, 215, 266
- Nieto J. L., Capaccioli M., Held E. V., 1988, *A&A*, 195, L1
- Omukai K., Schneider R., Haiman Z., 2008, *ApJ*, 686, 801
- Onken C. A., Ferrarese L., Merritt D., Peterson B. M., Pogge R. W., Vestergaard M., Wandel A., 2004, *ApJ*, 615, 645
- Ostriker J. P., Heisler J., 1984, *ApJ*, 278, 1
- Pacucci F., Narayan R., 2024, *ApJ*, 976, 96
- Pacucci F., Nguyen B., Carniani S., Maiolino R., Fan X., 2023, *ApJ*, 957, L3
- Pandey S., et al., 2024, *ApJ*, 976, 116
- Park D., Woo J.-H., Bennert V. N., Treu T., Auger M. W., Malkan M. A., 2015, *ApJ*, 799, 164
- Pascale R., Nipoti C., Calura F., Della Croce A., 2024, *A&A*, 684, L19
- Pechetti R., et al., 2022, *ApJ*, 924, 48
- Peng C. Y., 2007, *ApJ*, 671, 1098
- Pensabene A., Carniani S., Perna M., Cresci G., Decarli R., Maiolino R., Marconi A., 2020, *A&A*, 637, A84
- Percival W. J., Cole S., Eisenstein D. J., Nichol R. C., Peacock J. A., Pope A. C., Szalay A. S., 2007, *MNRAS*, 381, 1053
- Pérez-Gallego J., et al., 2011, *MNRAS*, 418, 2350
- Pérez-González P. G., et al., 2024, *ApJ*, 968, 4
- Peterson B. M., 1993, *PASP*, 105, 247
- Pfeffer J., Baumgardt H., 2013, *MNRAS*, 433, 1997
- Phillipps S., Drinkwater M. J., Gregg M. D., Jones J. B., 2001, *ApJ*, 560, 201
- Poci A., McDermid R. M., Zhu L., van de Ven G., 2019, *MNRAS*, 487, 3776
- Portegies Zwart S. F., McMillan S. L. W., 2002, *ApJ*, 576, 899
- Preto M., Amaro-Seoane P., 2010, *ApJ*, 708, L42
- Randall S. W., et al., 2015, *ApJ*, 805, 112
- Reines A. E., Volonteri M., 2015, *ApJ*, 813, 82
- Reines A. E., Greene J. E., Geha M., 2013, *ApJ*, 775, 116
- Reynolds J. H., 1925, *MNRAS*, 85, 1014
- Richings A. J., Uttley P., Körding E., 2011, *MNRAS*, 415, 2158
- Rinaldi P., et al., 2024, *arXiv e-prints*, p. arXiv:2411.14383
- Romanishin W., Strom K. M., Strom S. E., 1977, in *Bulletin of the American Astronomical Society*, p. 347
- Roos N., Norman C. A., 1979, *A&A*, 76, 75
- Rusli S. P., Thomas J., Erwin P., Saglia R. P., Nowak N., Bender R., 2011, *MNRAS*, 410, 1223
- Ryu T., Tanaka T. L., Perna R., Haiman Z., 2016, *MNRAS*, 460, 4122
- Sahu N., Graham A. W., Davis B. L., 2019, *ApJ*, 876, 155
- Sahu N., Graham A. W., Davis B. L., 2020, *ApJ*, 903, 97
- Sahu N., Graham A. W., Hon D. S. H., 2023, *MNRAS*, 518, 1352
- Salucci P., Ratnam C., Monaco P., Danese L., 2000, *MNRAS*, 317, 488
- Sandage A., Binggeli B., Tammann G. A., 1985, *AJ*, 90, 1759
- Saulder C., van den Bosch R. C. E., Mieske S., 2015, *A&A*, 578, A134
- Savorgnan G. A. D., Graham A. W., 2016a, *ApJS*, 222, 10
- Savorgnan G. A. D., Graham A. W., 2016b, *MNRAS*, 457, 320
- Savorgnan G. A. D., Graham A. W., Marconi A., Sani E., 2016, *ApJ*, 817, 21
- Sawangwit U., Shanks T., Abdalla F. B., Cannon R. D., Croom S. M., Edge A. C., Ross N. P., Wake D. A., 2011, *MNRAS*, 416, 3033
- Schawinski K., et al., 2014, *MNRAS*, 440, 889
- Schmidt M., 1963, *Nature*, 197, 1040
- Schweizer F., Seitzer P., 1992, *AJ*, 104, 1039
- Scorza C., Bender R., 1995, *A&A*, 293, 20
- Scorza C., van den Bosch F. C., 1998, *MNRAS*, 300, 469
- Scott N., Graham A. W., Schombert J., 2013, *ApJ*, 768, 76
- Serra P., et al., 2019, *A&A*, 628, A122
- Seth A. C., et al., 2014, *Nature*, 513, 398
- Shankar F., et al., 2016, *MNRAS*, 460, 3119
- Shao Y., et al., 2017, *ApJ*, 845, 138
- Shi F., Kong X., Li C., Cheng F. Z., 2005, *A&A*, 437, 849
- Sil'chenko O., 2013, *Memorie della Societa Astronomica Italiana Supplementi*, 25, 93
- Sil'chenko O. K., Afanasiev V. L., Chavushyan V. H., Valdes J. R., 2002, *ApJ*, 577, 668
- Spaans M., Silk J., 2006, *ApJ*, 652, 902
- Spitzer L. J., Baade W., 1951, *ApJ*, 113, 413
- Stickel M., Rieke G. H., Kuehr H., Rieke M. J., 1996, *ApJ*, 468, 556
- Suh H., et al., 2024, *arXiv e-prints*, p. arXiv:2405.05333
- Tan J. C., Singh J., Cammelli V., Sanati M., Petkova M., Nandal D., Monaco P., 2024, *arXiv e-prints*, p. arXiv:2412.01828
- Terrazas B. A., Bell E. F., Henriques B. M. B., White S. D. M., Cattaneo A., Woo J., 2016, *ApJ*, 830, L12
- Terrazas B. A., Bell E. F., Woo J., Henriques B. M. B., 2017, *ApJ*, 844, 170
- Toomre A., 1977, in *Tinsley B. M., Larson Richard B. Gehret D. C., eds, Evolution of Galaxies and Stellar Populations*. p. 401, doi:10.1146/annurev.aa.15.090177.002253
- Trujillo I., Ferré-Mateu A., Balcells M., Vazdekis A., Sánchez-Blázquez P., 2014, *ApJ*, 780, L20
- Übler H., et al., 2023, *A&A*, 677, A145
- Umemura M., Loeb A., Turner E. L., 1993, *ApJ*, 419, 459
- Venemans B. P., Walter F., Zschaechner L., Decarli R., De Rosa G., Findlay J. R., McMahon R. G., Sutherland W. J., 2016, *ApJ*, 816, 37
- Vestergaard M., Peterson B. M., 2006, *ApJ*, 641, 689
- Volonteri M., Rees M. J., 2005, *ApJ*, 633, 624
- Walsh J. L., van den Bosch R. C. E., Gebhardt K., Yildirim A., Gültekin K., Husemann B., Richstone D. O., 2015, *ApJ*, 808, 183
- Wandel A., 1999, *ApJ*, 519, L39
- Wang R., et al., 2010, *ApJ*, 714, 699
- Wang R., et al., 2013, *ApJ*, 773, 44
- Wang R., et al., 2016, *ApJ*, 830, 53
- Webster R. L., Francis P. J., Peterson B. A., Drinkwater M. J., Masci F. J., 1995, *Nature*, 375, 469
- Willott C. J., Bergeron J., Omont A., 2015, *ApJ*, 801, 123
- Willott C. J., Bergeron J., Omont A., 2017, *ApJ*, 850, 108
- Wolf C., Lai S., Onken C. A., Amrutha N., Bian F., Hon W. J., Tisserand P., Webster R. L., 2024, *Nature Astronomy*, 8, 520
- Yıldırım A., van den Bosch R. C. E., van de Ven G., Husemann B., Lyubenova M., Walsh J. L., Gebhardt K., Gültekin K., 2015, *MNRAS*, 452, 1792
- Yuan W., Zhou H., Dou L., Dong X. B., Fan X., Wang T. G., 2014, *ApJ*, 782, 55
- Yue M., Eilers A.-C., Ananna T. T., Panagiotou C., Kara E., Miyaji T., 2024, *ApJ*, 974, L26
- Zinnecker H., Keable C. J., Dunlop J. S., Cannon R. D., Griffiths W. K., 1988, in *Grindlay J. E., Philip A. G. D., eds, IAU Symposium Vol. 126, The Harlow-Shapley Symposium on Globular Cluster Systems in Galaxies*. p. 603
- Zwicky F., Kowal C. T., 1968, "Catalogue of Galaxies and of Clusters of Galaxies", Volume VI. California Institute of Technology, Pasadena
- Zwicky F., Zwicky M. A., 1971, *Catalogue of selected compact galaxies and of post-eruptive galaxies*. Guemligen, Switzerland
- de Martino I., Chakrabarty S. S., Cesare V., Gallo A., Ostorero L., Diaferio A., 2020, *Universe*, 6, 107
- de Vaucouleurs G., 1961, *ApJS*, 5, 233
- de Vaucouleurs G., de Vaucouleurs A., 1972, *MNRAS*, 77, 1
- den Brok M., et al., 2015, *ApJ*, 809, 101
- van Dokkum P. G., et al., 2008, *ApJ*, 677, L5
- van den Bergh S., 1976, *ApJ*, 206, 883
- van den Bosch R. C. E., Gebhardt K., Gültekin K., van de Ven G., van der Wel A., Walsh J. L., 2012, *Nature*, 491, 729